

## Anthropogenic Impacts on the Atmosphere

**Natural and anthropogenically-influenced isoprene  
oxidation in the Southeastern U.S.A. and central Amazon**

Lindsay D. Yee, Gabriel Isaacman-VanWertz, Rebecca Wernis, Nathan M Kreisberg, Marianne Glasius, Matthieu Riva, Jason Douglas Surratt, Suzane S de Sa, Scot T. Martin, M. Lizabeth Alexander, Brett B Palm, Weiwei Hu, Pedro Campuzano-Jost, Douglas A. Day, Jose L. Jimenez, Yingjun Liu, Pawel K. Misztal, Paulo Artaxo, Juarez Viegas, Antonio Manzi, Rodrigo Augusto Ferreira de Souza, Eric S. Edgerton, Karsten Baumann, and Allen H. Goldstein

*Environ. Sci. Technol.*, Just Accepted Manuscript • Publication Date (Web): 09 Apr 2020

Downloaded from [pubs.acs.org](https://pubs.acs.org) on April 9, 2020

**Just Accepted**

"Just Accepted" manuscripts have been peer-reviewed and accepted for publication. They are posted online prior to technical editing, formatting for publication and author proofing. The American Chemical Society provides "Just Accepted" as a service to the research community to expedite the dissemination of scientific material as soon as possible after acceptance. "Just Accepted" manuscripts appear in full in PDF format accompanied by an HTML abstract. "Just Accepted" manuscripts have been fully peer reviewed, but should not be considered the official version of record. They are citable by the Digital Object Identifier (DOI®). "Just Accepted" is an optional service offered to authors. Therefore, the "Just Accepted" Web site may not include all articles that will be published in the journal. After a manuscript is technically edited and formatted, it will be removed from the "Just Accepted" Web site and published as an ASAP article. Note that technical editing may introduce minor changes to the manuscript text and/or graphics which could affect content, and all legal disclaimers and ethical guidelines that apply to the journal pertain. ACS cannot be held responsible for errors or consequences arising from the use of information contained in these "Just Accepted" manuscripts.

	Science, Policy, and Management

SCHOLARONE™  
Manuscripts

1    Natural and anthropogenically-influenced isoprene  
2    oxidation in the Southeastern U.S.A. and central  
3    Amazon

4    AUTHOR NAMES

5    *Lindsay D. Yee,<sup>†,\*</sup> Gabriel Isaacman-VanWertz,<sup>†,a</sup> Rebecca A. Wernis,<sup>§</sup> Nathan M. Kreisberg,<sup>‡</sup>  
6    Marianne Glasius,<sup>♦</sup> Matthieu Riva,<sup>○,b</sup> Jason D. Surratt,<sup>○</sup> Suzane S. de Sá,<sup>〃</sup> Scot T. Martin,<sup>〃,L</sup> M.  
7    Lizabeth Alexander,<sup>#</sup> Brett. B. Palm,<sup>〃,c</sup> Weiwei Hu,<sup>〃</sup> Pedro Campuzano-Jost,<sup>〃</sup> Douglas A. Day,  
8    <sup>〃</sup> Jose L. Jimenez,<sup>〃</sup> Yingjun Liu,<sup>〃,d</sup> Pawel K. Misztal,<sup>†,e</sup> Paulo Artaxo,<sup>〃</sup> Juarez Viegas,<sup>♦</sup> Antonio  
9    Manzi,<sup>♦</sup> Rodrigo A. F. de Souza,<sup>∞</sup> Eric S. Edgerton,<sup>¶</sup> Karsten Baumann,<sup>¶,f</sup> and Allen H.  
10   Goldstein<sup>†,§,\*</sup>*

11   AUTHOR ADDRESS

12   <sup>†</sup>Department of Environmental Science, Policy, and Management, University of California,  
13   Berkeley, California 94720, United States

14   <sup>§</sup>Department of Civil and Environmental Engineering, University of California, Berkeley,  
15   California 94720, United States

16   <sup>‡</sup>Aerosol Dynamics Inc., Berkeley, California 94710, United States

- 17   <sup>\*</sup>Department of Chemistry, Aarhus University, 8000 Aarhus C, Denmark
- 18   <sup>o</sup>Department of Environmental Sciences and Engineering, Gillings School of Global Public
- 19   Health, University of North Carolina, Chapel Hill, North Carolina 27599, United States
- 20   <sup>l</sup>School of Engineering and Applied Sciences, Harvard University, Cambridge, Massachusetts
- 21   01451, United States
- 22   <sup>t</sup>Department of Earth and Planetary Sciences, Harvard University, Cambridge, Massachusetts
- 23   01451, United States
- 24   <sup>#</sup>Environmental Molecular Sciences Laboratory, Pacific Northwest National Laboratory,
- 25   Richland, Washington 99352, United States
- 26   <sup>v</sup>Department of Chemistry & Biochemistry and Cooperative Institute for Research in
- 27   Environmental Sciences (CIRES), University of Colorado, Boulder, Colorado 80309, United
- 28   States
- 29   <sup>u</sup>Universidade de São Paulo, São Paulo, Brazil, 05508-020
- 30   <sup>♦</sup>Instituto Nacional de Pesquisas da Amazonia, Manaus, Amazonas, Brazil, 69060-001
- 31   <sup>¶</sup>Atmospheric Research & Analysis, Inc., Cary, North Carolina 27513, United States
- 32   <sup>o</sup>Universidade do Estado do Amazonas, Manaus, Amazonas, Brazil, 69735-000
- 33

34 ABSTRACT

35 Anthropogenic emissions alter secondary organic aerosol (SOA) formation chemistry from  
36 naturally emitted isoprene. We use correlations of tracers and tracer ratios to provide new  
37 perspectives on sulfate, NO<sub>x</sub>, and particle acidity influencing isoprene-derived SOA in two  
38 isoprene-rich forested environments representing clean to polluted conditions—wet and dry  
39 seasons in central Amazonia and Southeastern U.S.A. summer. We used the Semi-Volatile  
40 Thermal desorption Aerosol Gas Chromatograph (SV-TAG) and filter collection to measure  
41 SOA tracers indicative of isoprene/HO<sub>2</sub> (2-methyltetrols, C<sub>5</sub>-alkene triols, 2-methyltetrol  
42 organosulfates) and isoprene/NO<sub>x</sub> (2-methylglyceric acid, 2-methylglyceric acid organosulfate)  
43 pathways. Summed concentrations of these tracers correlated with particulate sulfate spanning  
44 three orders of magnitude, suggesting that 1  $\mu\text{g m}^{-3}$  reduction in sulfate corresponds with at least  
45 ~0.5  $\mu\text{g m}^{-3}$  reduction in isoprene-derived SOA. We also find that isoprene/NO<sub>x</sub> pathway SOA  
46 mass is primarily comprised of organosulfates, ~97% in the Amazon and ~55% in the  
47 Southeastern U.S. We infer under natural conditions in high isoprene emission regions,  
48 preindustrial aerosol sulfate was almost exclusively isoprene-derived organosulfates, which are  
49 traditionally thought as representative of anthropogenic influence. We further report the first  
50 field observations showing that particle acidity correlates positively with 2-methylglyceric acid  
51 partitioning to the gas phase and negatively with the ratio of 2-methyltetrols to C<sub>5</sub>-alkene triols.

52 **Introduction**

53 Isoprene-derived carbon contributes significantly to the global secondary organic aerosol (SOA)  
54 budget.<sup>1</sup> As such it contributes to global impacts of SOA including air quality, adverse human  
55 health effects, and affecting Earth's radiative balance. SOA formed from oxidation of biogenic

56 volatile organic compounds (VOCs), such as isoprene, is enhanced by anthropogenic pollutants  
57 including NO<sub>x</sub>, SO<sub>2</sub>, O<sub>3</sub>, black carbon, and particulate matter.<sup>2–7</sup> Still, atmospheric measurements  
58 constraining chemical mechanisms and understanding of the extent by which these chemical levers  
59 affect isoprene-derived SOA formation are limited.<sup>8–14</sup> The anthropogenic impact of NO<sub>x</sub> and SO<sub>2</sub>  
60 (as a precursor to particulate sulfate) on SOA formation from isoprene has been investigated  
61 extensively in the laboratory.<sup>2,3,15–20</sup> NO<sub>x</sub> ultimately controls the branching ratio between different  
62 chemical pathways to SOA derived from isoprene (referenced hereafter as isoprene-SOA), and  
63 particulate sulfate facilitates the reactive uptake of isoprene-derived gas-phase intermediates.<sup>5,21–</sup>  
64 <sup>23</sup> Sulfate also affects particle liquid water content and particle pH, all of which affect the  
65 physicochemical conditions under which isoprene-SOA forms.<sup>8,24–29</sup>

66 Isoprene reacts primarily with OH radicals during daytime forming an isoprene peroxy radical.  
67 At sufficiently low NO<sub>x</sub> levels (referenced as isoprene/HO<sub>2</sub> pathway), an isoprene hydroperoxide  
68 (ISOPOOH) is formed, and subsequent oxidation of ISOPOOH with an OH radical results in  
69 rearrangement to gas-phase isoprene epoxydiol (IEPOX) isomers.<sup>30</sup> Under these conditions,  
70 isoprene-SOA derives primarily from acid-catalyzed multiphase chemistry of IEPOX involving  
71 uptake into the aqueous phase of particulate matter,<sup>21,22,27,30–33</sup> and this SOA is referred to as  
72 IEPOX-SOA. IEPOX-SOA is estimated to contribute up to 30% of OA across many sites  
73 worldwide.<sup>7,34</sup> Several molecular tracers of IEPOX-SOA previously measured in laboratory/field  
74 include: 2-methyltetros and their oligomers,<sup>21,35–37</sup> C<sub>5</sub>-alkene triols,<sup>15,16,38,39</sup> methyl  
75 tetrahydrofurans, and methyltetrol sulfates.<sup>5,21,24,40–42</sup> These molecular tracers (all isomers listed  
76 **Table S2**) will be respectively referred to in the rest of this paper as: 2-MTs, C5ALKTRIOLS,  
77 THFs, and MT-OSSs. Oligomers formed from some of these tracers have been observed,<sup>15</sup> although

78 their mass contribution remains unconstrained, and they may decompose during thermal  
79 desorption analysis contributing to the observed tracers.<sup>42–45</sup>

80 The presence of higher levels of NO<sub>x</sub> (referenced as isoprene/NO<sub>x</sub> pathway) leads to a parallel  
81 route of SOA formation from oxidation of methacrolein (MACR),<sup>17,21,46</sup> referred here as MACR-  
82 SOA. Oxidation of MACR forms methacryloyl peroxy nitrate (MPAN), which further oxidizes to  
83 methacrylic epoxide (MAE)<sup>47</sup> and hydroxyl methyl methyl lactone (HMML).<sup>48</sup> Multiphase  
84 chemistry of MAE/HMML leads to 2-methylglyceric acid (2-MG), 2-methylglyceric acid  
85 organosulfate (2-MG-OS), and their respective oligomeric forms.<sup>15,49,50</sup> This route is typically less  
86 efficient in SOA formation compared to IEPOX-SOA route because MPAN survival in the  
87 atmosphere is strongly enhanced at lower temperatures while isoprene emissions increase  
88 exponentially with temperature. Thus, reaction with OH must occur on a timescale competitive to  
89 MPAN decomposition to sufficiently form MACR-SOA intermediates.<sup>51</sup>

90 Field observations spanning clean to polluted conditions are sparse<sup>36</sup> but important for  
91 examining correlations between molecular markers of isoprene-SOA and chemical levers on OA  
92 chemistry (e.g. NO<sub>x</sub>, particulate sulfate, and particle pH). Here, we made measurements in two  
93 similar, though unique environments (Southeast United States and central Amazon) to examine  
94 isoprene chemistry over such atmospheric conditions. Each region is high in isoprene emissions,  
95 yet with differing histories and trajectories of anthropogenic influence. Previous measurements in  
96 another region of the Amazon Basin (Rondônia, Brazil) included offline filter-based measurement  
97 of isoprene/HO<sub>x</sub> tracers, 2-MTs and C5ALKTRIOLS.<sup>36</sup> Here we report in situ measurement of  
98 these tracers in addition to isoprene/NO<sub>x</sub> tracer 2-MG in both gas and particle phases, as well as  
99 offline filter-based measurements of isoprene-derived organosulfates, MT-OSs and 2-MG-OS.  
100 Through correlation analyses utilizing this newly available higher time resolution tracer and

101 particle composition data, we further specify the role of particle acidity and the extent by which  
102 anthropogenically- *and* naturally-derived NO<sub>x</sub> and sulfate promote their formation, affect tracer  
103 ratios, and determine their gas/particle partitioning.

104 **Materials and Methods**

105 This work relies primarily on data collected using a Semi-Volatile Thermal desorption Aerosol  
106 Gas Chromatograph (SV-TAG) and a suite of supporting instrumentation at two field sites over  
107 three campaigns. Measurements were conducted at the Centreville, Alabama, U.S.A. site during  
108 the Southern Oxidant and Aerosol Study 2013 (SOAS)<sup>52</sup> and downwind of Manaus, Brazil “T3”  
109 site during the Green Ocean Amazon (GoAmazon 2014/5) field campaigns.<sup>53,54</sup> SOAS took place  
110 from 1 Jun 2013 to 15 Jul 2013. For GoAmazon 2014/5, measurements reported herein took place  
111 from 1 Feb to 26 Mar 2014, known as the first Intensive Operating Period 1 (IOP1) and referred  
112 to hereafter as “wet season”, and from 15 Aug to 15 Oct 2014, known as IOP2 and referred to  
113 hereafter as “dry season.” Both sites represent areas of high isoprene emissions affected by urban  
114 centers (i.e. Birmingham, Alabama, for Centreville and Manaus, Amazonas for “T3”). Manaus  
115 plume impacted sampled air masses at “T3” ~40% (wet season) and ~60% (dry season) of the  
116 time. The dry season is further characterized by an enhancement in regional biomass burning  
117 influences.<sup>54,55</sup>

118 SV-TAG provided gas and particle phase speciation of semi-volatile organic compounds, an  
119 Aerodyne Aerosol Mass Spectrometer (AMS) provided PM<sub>1</sub> organic and inorganic speciation, and  
120 quartz filter analysis provided speciation of OSs in PM<sub>2.5</sub> samples collected during SOAS and PM<sub>1</sub>  
121 filter samples collected during GoAmazon. An Ionicon Proton Transfer Mass Spectrometer  
122 (PTRMS) measured gas-phase concentrations of isoprene. Instrument operation, analysis, and

123 deployment details during these field campaigns were published for SV-TAG,<sup>43,56,57</sup> AMS,<sup>13,58,59</sup>  
124 particulate filter collection and OSs analysis by liquid chromatography coupled to electrospray  
125 ionization high-resolution mass spectrometry (LC/ESI-HR-MS),<sup>14,57,60,61</sup> and PTRMS.<sup>62,63</sup>  
126 Synthesized MT-OSs were analyzed by SV-TAG to estimate degree of their decomposition during  
127 analysis; roughly < 10% of measured 2-MTs and C5ALKTRIOLS are formed through  
128 decomposition of MT-OSs, for details see Supporting Information. Model results for particle pH  
129 and liquid water content (LWC) are the same as used by Isaacman-VanWertz et al.,<sup>43</sup> utilizing the  
130 thermodynamic model ISORROPIA-II.<sup>64</sup> During SOAS, meteorological data (temperature,  
131 relative humidity, wind direction) and concentrations of NO<sub>x</sub>, NO<sub>y</sub>, and O<sub>3</sub> were measured within  
132 the SouthEastern Aersol Research and Characterization Network (SEARCH).<sup>65</sup> During  
133 GoAmazon, these parameters were measured within the co-located U.S. Department of Energy  
134 Atmospheric Radiation Measurement Climate Facility comprising Atmospheric Radiation  
135 Measurement Facility One (AMF-1) and Mobile Aerosol Observation System (MAOS).<sup>66</sup>

## 136 Results and Discussion

### 137 1. Field campaign comparisons

138 Concentration ranges from GoAmazon wet/dry season and SOAS for isoprene, PM<sub>1</sub> organic,  
139 sulfate, and daytime NO<sub>y</sub> (representative of photochemical conditions and processed NO<sub>x</sub>) are  
140 summarized (**Figure S1**). GoAmazon wet season median concentrations are lowest, representing  
141 the least polluted and lowest aerosol loading conditions, though median NO<sub>y</sub> was only slightly  
142 lower with similar range as other measurement campaigns. GoAmazon dry season is characterized  
143 with higher biogenic emissions, regional biomass burning emissions, and less wet deposition,<sup>55</sup>  
144 having highest PM<sub>1</sub> organic although between wet season and SOAS for isoprene and sulfate.

145 SOAS exhibits highest anthropogenic influence (sulfate) and highest isoprene concentrations.  
146 Median NO<sub>y</sub> concentration during SOAS is slightly higher than the other campaigns, though  
147 narrow in range suggesting fewer large local emission sources and a more regionally averaged  
148 contribution sampled in this rural region of Alabama. The greater range of observed NO<sub>y</sub> values  
149 during GoAmazon reflects pollution plumes influencing local chemistry.<sup>67</sup> We note that while  
150 more polluted on average than GoAmazon, SOAS pollution levels were in fact the lowest since  
151 measurements began in 1999 for that region.<sup>68</sup> Mean temperature (*T*) and relative humidity (RH)  
152 during corresponding measurement times were: SOAS  $T_{\text{mean}} = 24.7 \text{ }^{\circ}\text{C}$ , RH<sub>mean</sub> = 82%; GoAmazon  
153 wet season  $T_{\text{mean}} = 26.5 \text{ }^{\circ}\text{C}$ , RH<sub>mean</sub> = 90%; GoAmazon dry season  $T_{\text{mean}} = 27.9 \text{ }^{\circ}\text{C}$ , RH<sub>mean</sub> = 83%.<sup>43</sup>

154 **2. Tracer correlations reveal chemical factors influencing isoprene chemistry**

155 The range of conditions for biogenic and anthropogenic emissions observed in these campaigns  
156 provides a useful opportunity to compare the chemical fate of isoprene during oxidation under  
157 clean versus polluted conditions. Temporal variability in SV-TAG measured molecular markers  
158 (particle-only and gas + particle) were compared with each other and several other  
159 calculated/measured parameters through correlation analyses. Coefficients of determination, R<sup>2</sup>,  
160 are summarized in **Table S3** for: SOAS; GoAmazon wet season; GoAmazon dry season; all  
161 datasets taken together. Many moderate correlations ( $R^2 \geq 0.4$ , values bolded in **Table S3**)  
162 between measured tracers and organic, sulfate, nitrate, and ozone concentrations within any one  
163 deployment period exist. When measurements from SOAS and both GoAmazon deployments are  
164 taken together, correlations for IEPOX-SOA tracers are still clearly strongest with sulfate ( $R^2 =$   
165 0.40). Taken individually, correlations of molecular markers of IEPOX-derived SOA tracers (i.e.  
166 2-MTs, C5ALKTRIOLS) with sulfate during GoAmazon are generally higher than previous  
167 analyses for other sites throughout the U.S.A.<sup>11,58</sup> This could derive from 1) owing to hourly

168 measurements by SV-TAG, increased time resolution may better capture dynamics of particle  
169 composition, and 2) a wide range in sulfate concentrations was measured across these  
170 deployments, revealing correlation with sulfate is strong across the whole range from polluted to  
171 extremely clean conditions, not just when anthropogenic pollution is abundant. Correlations of  
172 tracers with particle pH and liquid water content (LWC) vary across different deployments from  
173 non-existent to moderate, and we further discuss these relationships in the context of isoprene-  
174 SOA formation.

175 **2A. Influence of sulfate on isoprene-SOA from clean to polluted conditions**

176 Many studies interpret enhancements in isoprene-SOA formation correlated with sulfate as  
177 indicative of isoprene-SOA formation enhanced by anthropogenically-derived sulfate.<sup>2,9,10,69</sup>  
178 Sulfate is cited as having a central role on influencing SOA formation from isoprene by enhancing  
179 uptake of IEPOX/MAE/HMML into the particle phase by affecting particle surface area,<sup>69</sup> as well  
180 as hygroscopicity and thereby LWC, aqueous particle volume,<sup>12,29,70,71</sup> and particle acidity.<sup>21,24,27,47</sup>  
181 It can also facilitate “salting in” conditions to enhance IEPOX uptake into the particle phase and  
182 directly reacts with epoxide intermediates to form organosulfates,<sup>5,47</sup> whereas the free acid form  
183 (sulfuric acid) serves as a catalyst in the hydrolysis of IEPOX to form 2-MTs.<sup>9,33</sup> It was surmised  
184 that sulfate is the limiting reagent in isoprene-SOA formation in the Southeast U.S.A. based on  
185 significant correlation between sulfate and estimated isoprene-derived SOA (positive matrix  
186 factorization analysis of AMS mass spectra).<sup>9,34</sup> While yields of several isoprene SOA molecular  
187 markers increases in the presence of particulate sulfate in acidic particles, atmospheric  
188 measurements reporting such strong correlations are limited to regions with significant  
189 anthropogenic pollution such as eastern U.S.A. and China.<sup>10,11,72</sup>

190 Here, we show that markers of both IEPOX-SOA and MACR-SOA correlate with ambient  
191 sulfate, but over a range of concentrations covering much cleaner conditions than previously  
192 reported.<sup>9,13,51,58</sup> Molecular tracers are well correlated even at concentrations of particulate sulfate  
193 < 0.5  $\mu\text{g m}^{-3}$  (**Figure 1**) representing Amazon basin background conditions and at times pre-  
194 industrial conditions.<sup>13,73–75</sup> In these environments, IEPOX-SOA tracers (2-MTs +  
195 C5ALKTRIOLS) (**Figure 1a**) contribute significantly more mass to SOA than MACR-SOA tracer  
196 (2-MG) (**Figure 1b**). IEPOX-SOA tracers correlate moderately with sulfate across all three  
197 campaigns (**Table S3**:  $R^2 = 0.48$ ; 0.49; 0.57; 0.40 for SOAS; wet season; dry season; all datasets,  
198 respectively), similar to or higher than previous reports of tracers<sup>10,11</sup> and IEPOX-SOA statistical  
199 factor.<sup>9,13,29,34</sup> 2-MG contributes more mass in SOAS data than GoAmazon but is only weakly  
200 correlated with sulfate during all campaigns (**Table S3**:  $R^2 < 0.25$  for each dataset). We keep in  
201 mind that correlations can also be affected by atmospheric transport including dispersion/dilution  
202 and wet deposition. Despite marginal correlation between 2-MG and sulfate and the offset in  
203 magnitude between SOAS and GoAmazon, we demonstrate that correlations are improved by  
204 accounting for OS formations.

## 205 **2B. OS formations differ by HO<sub>2</sub>/NO<sub>x</sub> pathway and environment**

206 OSs formed from chemical reaction of isoprene-derived intermediates and sulfate in the aqueous  
207 phase contribute a substantial fraction of isoprene-SOA.<sup>14,41,42,61,76–78</sup> Here, OS analysis included  
208 MT-OSs from IEPOX (“OS-216”),<sup>5,21,22</sup> and 2-MG-OS (“OS-200”), which can be derived along  
209 MACR-SOA (isoprene/NO<sub>x</sub>) pathway from 2-MG<sup>5</sup> and HMML/MAE.<sup>47</sup> We explore the relative  
210 distribution of the isoprene-derived SOA organic carbon mass in molecular tracers measured by  
211 SV-TAG, versus OS forms (offline filter analysis).

212 Summed particle-phase isoprene-SOA tracers (SV-TAG molecular tracers and OSs organic  
213 carbon) contribute on average 11%, 13%, and 14% of total PM<sub>1</sub> organic mass for SOAS,  
214 GoAmazon wet season, and GoAmazon dry season, respectively. **Figure 2** shows the distribution  
215 of isoprene-SOA tracers, including OSs across the three deployments. For IEPOX-SOA pathway,  
216 similar fractions as MT-OSs are present across all campaigns (23-28%), leading to similar trends  
217 between data in **Figure 1a** and **Figure 1c** (summation of 2-MTs, C5ALKTRIOLS, and MT-OSs  
218 organic carbon) but with a vertical offset. Similar correlation with sulfate (**Table S3**; R<sup>2</sup> = 0.41  
219 accounting for OSs vs R<sup>2</sup> = 0.40 excluding OSs) is observed. **Figure 2** shows that MACR-SOA  
220 pathway is only a few percent of observed isoprene-SOA. However, most MACR-SOA pathway  
221 mass during GoAmazon is bound with sulfate as 2-MG-OS, whereas in SOAS the distribution is  
222 almost even between 2-MG and 2-MG-OS. Thus, combining 2-MG-OS organic mass with 2-MG  
223 (**Figure 1d**) increases total accounted MACR-SOA by more than an order of magnitude for  
224 GoAmazon data than that accounted in **Figure 1b**, revealing sulfate as an important nucleophile  
225 in MACR-SOA formation as well. Accounting for GoAmazon 2-MG-OS carbon, correlation of  
226 MACR-SOA tracers with sulfate (**Table S5**; R<sup>2</sup> = 0.33) is slightly improved (**Table S3**; R<sup>2</sup> < 0.25  
227 each dataset), comparable to previous reports (R<sup>2</sup> ≤ 0.33),<sup>10,11,72</sup> but extended here to levels of  
228 sulfate < 1 μg m<sup>-3</sup>. The correlation is in fact much stronger than previous reports<sup>10,11,72</sup> if data with  
229 sulfate ≤ 1 μg m<sup>-3</sup> are considered (**Table S5**; R<sup>2</sup> = 0.66), as there may be a threshold in MACR-  
230 SOA at >1 μg m<sup>-3</sup> sulfate concentrations. In contrast, there is no apparent threshold for IEPOX-  
231 SOA over the sulfate concentrations observed. Since previous observations of MACR-SOA  
232 correlation with sulfate are typically reported for conditions with sulfate concentrations > 1 μg m<sup>-3</sup>,  
233 this could be why the role of sulfate on MACR-SOA pathway has been less clear by R<sup>2</sup>. Further,  
234 although sulfate and 2-MG levels are higher during SOAS than during GoAmazon (**Figure S1** and

235 **Figure 1**), lower 2-MG-OS fraction may result from higher sulfate and free acidity in hydrated  
236 particles leading to hydrolysis of 2-MG-OS to 2-MG.<sup>48</sup> With increasing acidity, 2-MG partitions  
237 to the gas phase (see Section 3A.), which may weaken the correlation with higher sulfate levels.  
238 Additional differences might include the relative yields of HMML/MAE formed from MACR<sup>79</sup> as  
239 2-MG precursors, phase state, morphology, or viscosity.

240 Linear regressions of data across all three deployments reflect different relationships between  
241 the IEPOX-SOA and MACR-SOA pathways with sulfate (**Figure 1**). Data in **Figure 1** were  
242 binned (five data points each), and a linear fit was performed on the means of all bins (**Figure S2**;  
243 **Table S4**; **Table S5**). Tracers of both formation pathways correlate with sulfate (IEPOX-SOA:  
244 slope =  $490.73 \pm 35$ ,  $R^2 = 0.88$ ; MACR-SOA: slope =  $5.70 \pm 1.28$ ,  $R^2 = 0.59$ ). Units of slopes are  
245 ng m<sup>-3</sup> of IEPOX or MACR-SOA tracers, respectively, per  $\mu\text{g m}^{-3}$  of particulate sulfate.  
246 GoAmazon data are situated within fairly distinct ranges of sulfate with little overlap (**Figure 1**).  
247 SOAS data, while typically within sulfate  $> 1 \mu\text{g m}^{-3}$ , does show a similar trend down to lower  
248 sulfate levels overlapping GoAmazon data for the case of IEPOX-SOA, but there is very little  
249 overlap in measurements from different deployments  $< 1 \mu\text{g m}^{-3}$  sulfate for MACR-SOA.

250 From an air quality perspective assuming that sulfate is a primary driver of isoprene-SOA  
251 formation,<sup>5,9,10,34,58,69,80</sup> these quantitative relationships suggest that every  $1 \mu\text{g m}^{-3}$  reduction in  
252 sulfate can lead to at least  $\sim 0.5 \mu\text{g m}^{-3}$  reduction of these tracers contributing to isoprene-SOA, at  
253 least over sulfate and NO<sub>y</sub> ranges observed here. Previous studies for Southeast U.S.A. also  
254 suggested that reductions in SO<sub>2</sub> (taken as reductions in sulfate) lead to significant decreases in  
255 SOA<sup>81</sup> from isoprene.<sup>9,12,26,29,69</sup> This idea is extended here to the measurements taken during  
256 GoAmazon wet season characterized by relatively low levels of sulfate, which can represent pre-  
257 industrial conditions, suggesting that natural sources of SO<sub>2</sub> also control SOA yield from isoprene

258 oxidation. For the Amazon basin, low “background” sulfate levels can be attributed to biogenic  
259 sources such as DMSO and H<sub>2</sub>S as well as long range transport of (anthropogenic) sulfate  
260 sources.<sup>13,73,75,82,83</sup> Higher sulfate levels were observed during GoAmazon dry season, some  
261 attributable to biomass burning<sup>84</sup> and not due to seasonal changes in anthropogenic activity at  
262 Manaus. We surmise that sulfate concentrations are higher relative to the wet season in part  
263 because there is less wet deposition due to precipitation and lower ventilation rates in the dry  
264 season. In contrast, higher concentrations of sulfate (some similar to levels observed during dry  
265 season of central Amazon) observed in the Southeast U.S.A. are reasonably attributable to  
266 anthropogenic activity.<sup>68,85</sup>

267 Overall, these results further corroborate aerosol sulfate as a strong determinant of isoprene-  
268 SOA formation over a wide range of environments. Importantly, though we find this correlation  
269 holds across three orders of magnitude down to low levels likely representative of pre-industrial  
270 conditions and revealed here to be true for the isoprene/NO<sub>x</sub> channel as well. While 2-MG-OS at  
271 SOAS is a reflection of anthropogenic influence from NO<sub>x</sub> and SO<sub>2</sub> emissions, natural NO<sub>x</sub>  
272 emissions in the Amazon are sufficient to sustain isoprene/NO<sub>x</sub> pathways to form MACR-SOA  
273 during the wet season.<sup>63</sup> This suggests that even background/natural isoprene-derived SOA is  
274 enhanced by natural sulfate, and that sulfate is likely the limiting reagent given plenty of gas-phase  
275 production of IEPOX and HMML/MAE for the isoprene/HO<sub>2</sub> and isoprene NO<sub>x</sub> channels,  
276 respectively. As Riva et al.<sup>14</sup> suggest for pristine central Amazon conditions, over 80% of inorganic  
277 sulfate converts to organosulfur via reaction with IEPOX. Further, GoAmazon particles can be  
278 more acidic compared to areas with greater anthropogenic NH<sub>3</sub>(g) emissions, promoting relatively  
279 greater OS formation from isoprene.<sup>61</sup> Thus, we infer that under natural conditions in regions with  
280 high isoprene emissions, preindustrial aerosol sulfate was likely almost exclusively OSs derived

281 from isoprene. Because OS and inorganic sulfate differ in water uptake properties,<sup>86,87</sup> this implies  
282 preindustrial aerosol sulfate (albeit less abundant) may have been less reflective than current  
283 models assume.

284 **3. Role of particle acidity**

285 While sulfate is known to affect and correlate with particle pH (**Figure S3**), the separate  
286 influence of particle acidity on isoprene-SOA formation remains unclear. Laboratory studies  
287 demonstrated particle acidity enhances IEPOX uptake<sup>24,27</sup> and MACR-SOA.<sup>48,88</sup> Higher dry  
288 season IEPOX-SOA tracers concentrations compared to those in wet and transition seasons of  
289 2002 in another region of the Amazon Basin were attributed in part to increased aerosol acidity by  
290 contrasting concentrations of acidic gases, sulfate, and nitrate anions.<sup>36</sup> Online measurements of  
291 PM<sub>1</sub> composition conducted here now allow for explicit correlations of these tracers with pH,  
292 though they are not found to be significantly correlated, **Table S3**), nor are appreciable differences  
293 in particle acidity between the seasons observed (**Figure S3**). This further supports that sulfate is  
294 a primary driver of the observed tracers concentrations as discussed before. Other field  
295 measurements of isoprene-SOA molecular markers show no significant correlations with  
296 calculated pH,<sup>10,11,51,89</sup> often ascribed to measurements within a small pH range and possible  
297 conflating effects of regional transport where calculated pH for conditions at a field site are not  
298 necessarily representative of aerosol acidity at the time/place where pH-dependent chemistry  
299 occurs. We also do not observe significant correlations between concentrations of individual  
300 IEPOX-SOA and MACR-SOA markers and pH (**Table S3**), except slight to moderate correlation  
301 when considering gas + particle 2-MG ( $R^2 = 0.45$ ; 0.37 for wet season; dry season). This revealed  
302 that for isoprene/NO<sub>x</sub> pathway, the distribution of 2-MG between gas and particle phases correlates

303 with pH. For isoprene/HO<sub>2</sub> pathway, we later reveal correlation between pH and the ratio of  
304 IEPOX-SOA markers, 2-MTs and C5ALKTRIOLS.

305 **3A. Particle acidity and liquid water content affects MACR-SOA phase distribution**

306 **Figure 3** shows that 2-MG mass fraction in particle phase,  $F_p$ , correlates with pH during  
307 GoAmazon dry season ( $R^2 = 0.55$ ). The particle-phase concentration is in fact relatively constant  
308 over a range of pH values (0-3) for all three datasets (**Figure S4**). However, when considering  
309 gas-phase concentration, calculated as the difference between SV-TAG total (gas + particle) and  
310 particle channels, there is a decrease with increasing pH most obvious during GoAmazon (**Figure**  
311 **S5**). That is, 2-MG increasingly partitions to gas phase with increasing acidity. No/weak  
312 correlations of 2-MG with acidity have otherwise been observed from other field studies in the  
313 U.S.A.,<sup>8,10,11,51</sup> possibly due to methods of utilizing filter-based measurements which can suffer  
314 from artifacts of gas-phase adsorption, averaging due to lower time-resolution, as well as field  
315 observations that typically fall within narrow pH ranges (often below pH=2). SOAS data lay in a  
316 narrow range of calculated pH (0.25-1.0) and exhibit wider variation though higher average  $F_p$   
317 values for the same pH range as in GoAmazon (**Figure 3**). The variation may be due to other  
318 factors of liquid water content, ion activity, organics, and phase that affect 2-MG accommodation  
319 for SOAS conditions. More highly viscous and coated organic particles could lead to less 2-MG  
320 repartitioning back to the gas phase, keeping  $F_p$  values higher than expected from 2-MG vapor  
321 pressure.<sup>43</sup> In contrast, GoAmazon conditions comprise wider ranges in particle acidity and LWC  
322 associated with changes in 2-MG concentrations and observed  $F_p$ . The strongest trend for SOAS  
323 2-MG is with LWC (**Figure S6**) revealed in the total (gas + particle) channel; total 2-MG decreases  
324 with increasing LWC, again mostly associated with a decreasing gas-phase concentration as  
325 associated decreases in particle phase 2-MG are more modest (**Figure S7**). These measurements

326 are first field observation of pH- and LWC-dependent 2-MG accommodation in accordance to  
327 laboratory measurements,<sup>48</sup> in which gaseous 2-MG concentrations were observed to increase in  
328 the headspace over increasingly acidic solutions. This also suggests that for particles that are more  
329 acidic, more carbon through MACR-SOA pathway recycles back to the gas-phase after  
330 MAE/HMML uptake if no limitations to gas-particle exchange exist. In other words, the extent to  
331 which the particle phase acts as a reservoir of NO<sub>x</sub>-derived organic species is pH dependent for  
332 GoAmazon conditions. This further implies that PM formation along this route may be minimized  
333 by decreasing particle pH as Nguyen et al.<sup>48</sup> proposed that hydrated particles with higher free  
334 acidity might favor monomeric 2-MG as well as hydrolyze sulfate and nitrate esters<sup>79</sup> leading to  
335 suppression of SOA growth. Still, many other SOA formation mechanisms are more efficient  
336 under acidic conditions.<sup>90</sup> Others demonstrate that while SO<sub>2</sub> controls have led to lower particulate  
337 sulfate in the Southeast U.S.A., PM has remained acidic.<sup>68,91</sup> While GoAmazon includes pre-  
338 anthropogenic sulfate levels much lower than those of SOAS, and can be more acidic (associated  
339 with higher gas-phase fraction of 2-MG), they are still sufficiently acidic to promote IEPOX and  
340 MAE/HMML uptake as well as 2-MG-OS formation. This suggests that isoprene-SOA formation  
341 from these pathways is sustained even under natural/background levels of sulfate and NO<sub>x</sub>, and  
342 control of anthropogenic SO<sub>2</sub> emissions (as a source of sulfate) remains most effective in limiting  
343 SOA formation from both pathways.

344 **3B. Tracer ratios correlations further reveal role of acidity**

345 To better understand chemical controls on distribution of isoprene-derived carbon between  
346 different pathways to isoprene-SOA formation, we examine ratios of the SV-TAG measured  
347 molecular tracers as correlated with other chemical parameters. In this section we do not include  
348 carbon associated with OSs because of coarser time resolution of these measurements that would

349 limit the robustness of correlations; we note that scaling tracer concentrations by an average OS  
350 contribution would not impact correlations. We first investigate isoprene/HO<sub>2</sub> pathway (i.e.  
351 summed 2-MTs and C5ALKTRIOLS) vs the isoprene/NO<sub>x</sub> pathway (i.e. 2-MG) as IEPOX-SOA  
352 markers:MACR-SOA markers. We further explore branching of IEPOX-SOA carbon between 2-  
353 MTs and C5ALKTRIOLS.

354 **3C. Isoprene/HO<sub>2</sub> vs Isoprene/NO<sub>x</sub> pathway tracers correlations**

355 Based on current understandings of isoprene + OH oxidation, it would be expected that the split  
356 between carbon associated with IEPOX-SOA and MACR-SOA pathways would be NO<sub>y</sub>  
357 dependent. We evaluate the ratio of IEPOX-SOA:MACR-SOA tracers, i.e. (2-MTs +  
358 C5ALKTRIOLS):(2-MG), as correlated with NO<sub>y</sub>. Using NO<sub>y</sub> as a surrogate for integrated  
359 exposure of sampled air masses to NO<sub>x</sub><sup>13,63,67</sup> we explore the IEPOX-SOA:MACR-SOA tracers  
360 ratio as a proxy for the branching ratio between isoprene/HO<sub>2</sub> vs isoprene/NO<sub>x</sub> pathways. While  
361 this ratio might be expected to decrease with increasing NO<sub>y</sub>, correlations were poor regardless of  
362 phase (**Table S3**). **Figure S8** (particle phase) and **Figure S9** (total) also show that IEPOX-  
363 SOA:MACR-SOA ratios vs NO<sub>y</sub> filtered for daytime hours are still poorly correlated and widely  
364 variable across deployments. Very weak, though higher R<sup>2</sup> values (~0.2 for GoAmazon) are found  
365 for IEPOX-SOA:MACR-SOA ratios vs O<sub>3</sub> (**Table S3**), consistent with total 2-MG correlating  
366 better with O<sub>3</sub> (R<sup>2</sup> > 0.3 and up to 0.66) than with NO<sub>y</sub> (no correlation). Correlation of 2-MG with  
367 O<sub>3</sub> (**Figure S10** and **Figure S11**) suggests that O<sub>3</sub> is a better indicator of airmass age than NO<sub>y</sub> and  
368 is further discussed in Supporting Information.

369 **3D. Isoprene/HO<sub>2</sub> tracers ratio is pH dependent**

370 Limited studies have probed chemical controls on relative yields of IEPOX-SOA tracers, 2-MTs  
371 and C5ALKTRIOLS.<sup>21,23,71</sup> Formation of C5ALKTRIOLS has been explained by acid-catalyzed  
372 ring opening of isoprene epoxydiols.<sup>38</sup> Recent work suggests some fraction derives from  
373 decomposition of OSs and their oligomers thereof in some analytical techniques,<sup>42</sup> which may be  
374 representative of a tendency for many of these tracers to be formed by (thermal) decomposition  
375 during analysis.<sup>44,45,92</sup> Testing of MT-OSs in SV-TAG (see Supporting Information) suggests they  
376 would be a minor contribution (< 10% by mass) to 2-MTs and C5ALKTRIOLS observed here.  
377 The extent to which a given compound represents a sampled atmospheric constituent versus a  
378 transformed product of analysis remains an active area of methodological research. Here, we use  
379 these tracers as useful known indicators of isoprene oxidation, and we evaluate the extent to which  
380 different compound classes represent different formation pathways and can provide insight into  
381 particle-formation chemistry.

382 Plots of 2-MTs vs C5ALKTRIOLS reveal that distribution of IEPOX-derived carbon (as inferred  
383 from slope of the best fit line) and correlation between these analytes varies across these  
384 deployments **Figure 4**. 2-MTs:C5ALKTRIOLS is 0.52 with  $R^2 = 0.16$  for SOAS (**Figure 4a**), 0.27  
385 with  $R^2 = 0.54$  for GoAmazon wet season (**Figure 4b**), and 0.17 with  $R^2 = 0.72$  for GoAmazon  
386 dry season (**Figure 4c**). The variability in ratio and correlation of these tracers indicate that these  
387 analytes derive from distinct chemical conditions and possibly from additional precursors besides  
388 IEPOX. For example, 2-MTs were observed in SOA generated from isoprene ozonolysis under  
389 laboratory conditions,<sup>60,93</sup> though correlations of 2-MTs with O<sub>3</sub> are too poor in these datasets to  
390 suggest it as a leading source (**Table S3**).

391 The strongest explanatory variable for 2-MTS:C5ALKTRIOLS is pH ( $R^2 = 0.14$  for GoAmazon  
392 wet season,  $R^2 = 0.42$  for GoAmazon dry season, **Table S3** and **Figure 4d**). No trend with pH is

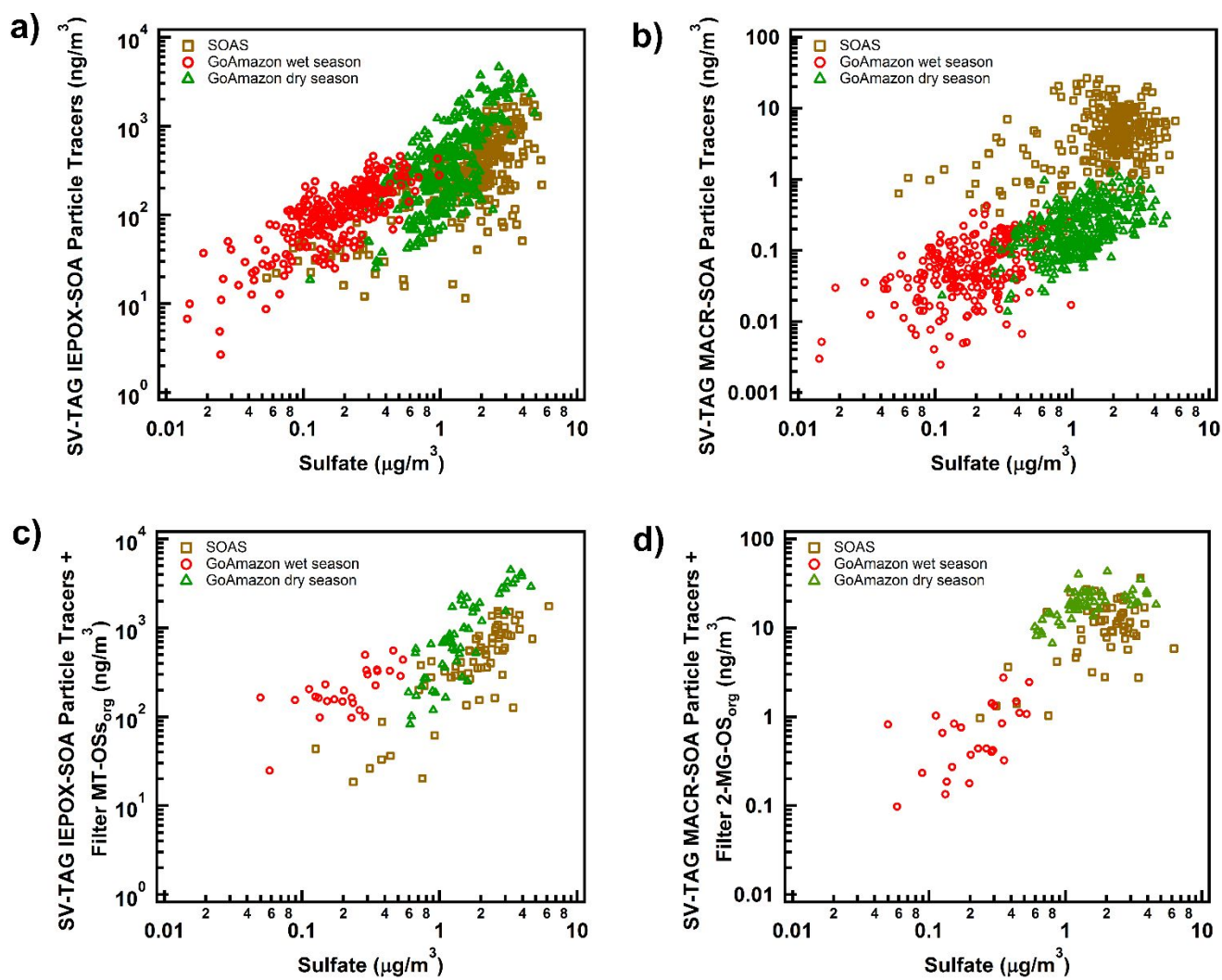
393 observed for SOAS and most data fall within  $\text{pH} = 0.5 \pm 0.5$ . This correlation was most obvious  
394 in GoAmazon datasets (**Figure 4**), where particle pH ranges more widely (0-3). As pH decreases,  
395 2-MTS:C5ALKTRIOLS also decreases suggesting that C5ALKTRIOLS formation is enhanced  
396 with increasing particle acidity (**Figure 4d**).<sup>38</sup> It is important to note that pH is a modeled output,  
397 and we keep in mind that the calculated pH values here result from assuming instantaneous gas-  
398 particle equilibrium. This assumption seems valid for liquid-phase organic aerosols observed in  
399 GoAmazon<sup>94</sup> and SOAS.<sup>95</sup> While RH and hence LWC can be highly variable as particles move  
400 about in daytime turbulence within the boundary layer, modeled pH may not reflect pH when  
401 IEPOX-SOA markers actually form, as limitations of the calculation have been discussed.<sup>13,43</sup>  
402 Still, we find that it is a useful metric for assessing particle-phase chemical conditions at the time  
403 these markers are measured. That is, concerted effects of RH,  $T$ , and gas/particle composition (e.g.  
404 sulfate, LWC, organics) is captured in calculated pH, and 2-MTS:C5ALKTRIOLS ratio serves as  
405 useful indicator of IEPOX-SOA formed under varying chemical conditions.

## 406 Atmospheric Implications

407 We provide the first ambient measurements revealing strong correlations with pH impacting  
408 tracer ratios derived in the isoprene/ $\text{HO}_2$  pathway (allowing for mechanistic insight) and phase  
409 partitioning of the isoprene/ $\text{NO}_x$  pathway tracer, 2-methylglyceric acid. Further, while the role of  
410 sulfate in isoprene-SOA formation has been studied, it has primarily been interpreted as a role of  
411 anthropogenically-derived sulfate enhancing SOA formation. We show here by contrasting SOAS  
412 and GoAmazon, that naturally-derived sulfate also enhances isoprene-SOA formation. In  
413 particular, the relatively greater incorporation of naturally-derived sulfate into organosulfates  
414 under the isoprene/ $\text{NO}_x$  channel during GoAmazon highlights the impact of more highly acidic  
415 particle conditions found in an environment representative of pre-industrial conditions, as well as

416 the fact that sulfate may be a stronger nucleophile than previously revealed for this  
417 pathway. Organosulfates are typically interpreted as markers of anthropogenic influence on SOA  
418 formation, which we demonstrate is not always the case, with implications for how such  
419 compounds are represented in global models of SOA and for the chemical composition and  
420 properties of pre-industrial SOA.

## 421 FIGURES



422

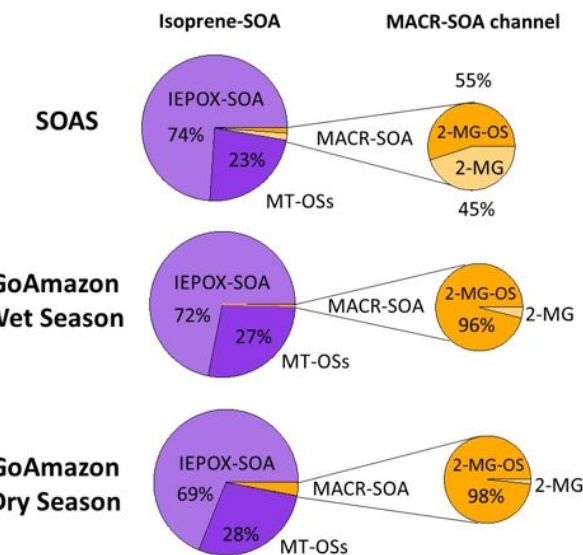
423 **Figure 1.** Particle-phase tracers from a) IEPOX and b) MACR channels of isoprene-SOA  
 424 formation as measured by SV-TAG and associated particulate sulfate as measured by AMS during  
 425 SOAS (brown squares), GoAmazon wet season (red circles), and GoAmazon dry season (green  
 426 triangles). Coefficients of determination,  $R^2 = 0.48; 0.49; 0.57; 0.40$  for SOAS; GoAmazon wet  
 427 season; GoAmazon dry season; all datasets, respectively, for a) IEPOX-SOA tracers correlated  
 428 with sulfate.  $R^2 < 0.25$  for each individual dataset and all datasets taken together for b) MACR-  
 429 SOA tracers correlated with sulfate. Summation of c) SV-TAG IEPOX-SOA particle-phase

430 tracers and filter MT-OSs organic and d) SV-TAG MACR-SOA particle-phase tracers and filter

431 2-MG-OS organic.

432

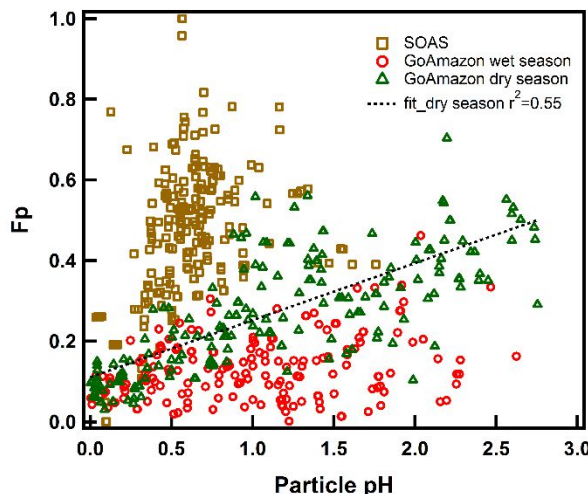
433



434

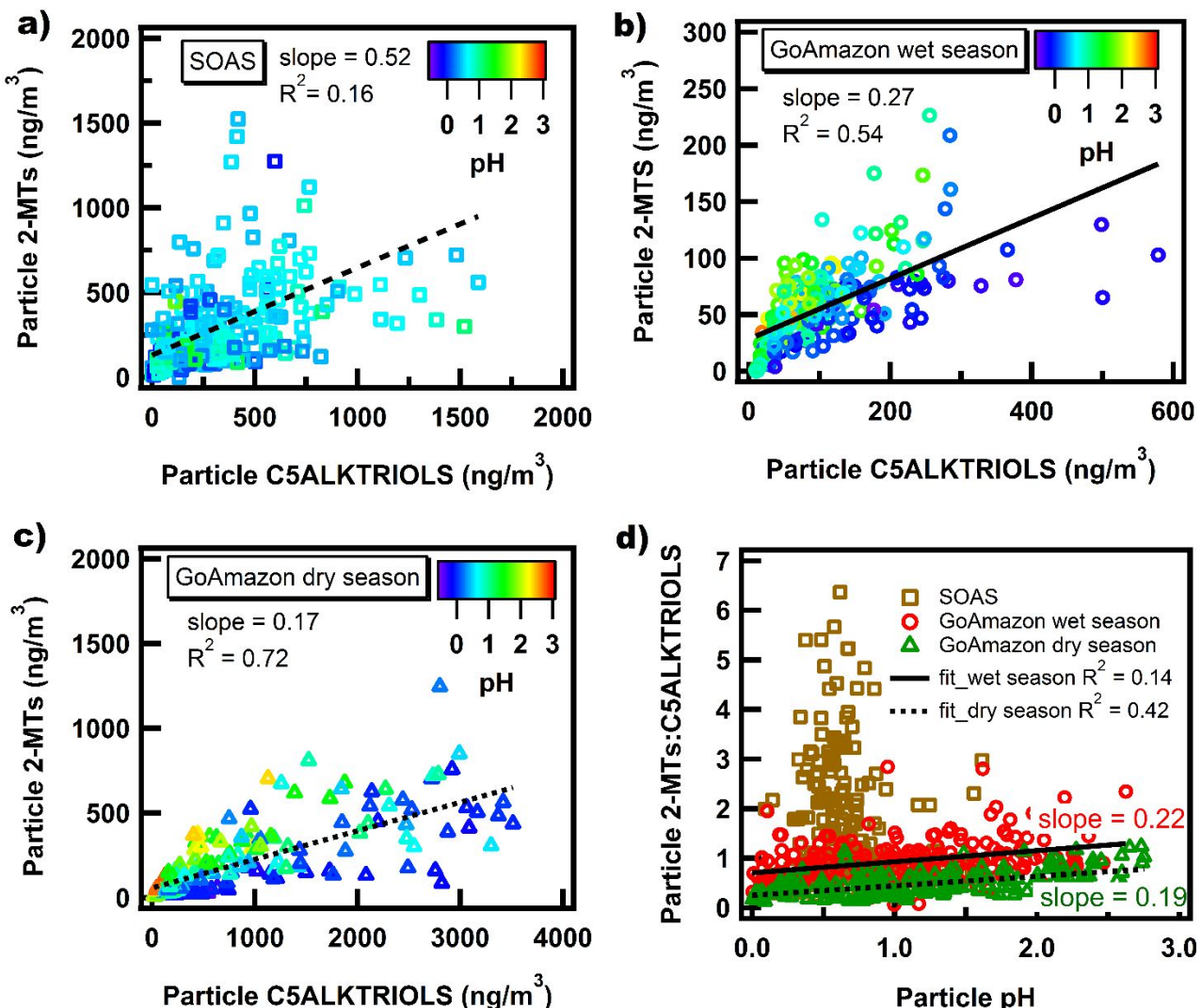
435 **Figure 2.** Distribution of isoprene-derived SOA mass between IEPOX-SOA (purple) molecular  
436 tracers: 2-MTs, C5ALKTRIOLS, and MT-OSs, and MACR-SOA (orange) molecular tracers: 2-  
437 MG and 2-MG-OS for SOAS (top), GoAmazon wet season (middle), and GoAmazon dry season  
438 (bottom).

439



440

441 **Figure 3.** Fraction of 2-MG in particle phase and associated particle pH during SOAS (brown  
442 squares), GoAmazon wet season (red circles), and GoAmazon dry season (green triangles). Data  
443 smoothed using a running-median smoothing algorithm. Best fit line (dashed) for GoAmazon dry  
444 season shown with slope = 0.14,  $R^2 = 0.55$ . Best fit lines for other campaigns not shown due to  
445 poor correlations ( $R^2 < 0.2$ ).



446

447 **Figure 4.** Particle phase 2-MTs vs C5ALKTRIOLS during a) SOAS, b) GoAmazon wet season,  
 448 and c) GoAmazon dry season. Best fit lines for each dataset shown along with slope and R<sup>2</sup>  
 449 values. Data are colored by particle pH, revealing some correlation of 2-MTs: C5ALKTRIOLS  
 450 with pH for GoAmazon datasets. Ratio of particle phase 2-MTs and C5ALKTRIOLS vs particle  
 451 pH in panel d) for SOAS (brown squares), GoAmazon wet season (red circles), and GoAmazon  
 452 dry season (green triangles). Best fit lines for GoAmazon wet season, solid line, slope = 0.22, R<sup>2</sup>  
 453 = 0.14 and GoAmazon dry season, dotted line, slope = 0.19, R<sup>2</sup> = 0.42 shown.

## 454 ASSOCIATED CONTENT

455 **Supporting Information.** The Supporting Information is available free of charge.

456 Additional details of Materials and Methods, figures of campaign comparisons, select tracer  
457 correlations, and a complete table of coefficients of determination for all calculated tracer  
458 correlations are included. (PDF)

## 459 AUTHOR INFORMATION

460 **Corresponding Author**

461 \* E-mail:lindsay.yee@berkeley.edu

462 \*E-mail:ahg@berkeley.edu

463 **Present Addresses**

464 <sup>a</sup>Now at Dept. of Civil and Environmental Engineering, Virginia Tech, Blacksburg, VA 24060,  
465 U.S.A.

466 <sup>b</sup>Now at Univ Lyon, Université Claude Bernard Lyon 1, CNRS, IRCELYON, F-69626,  
467 Villeurbanne, France

468 <sup>c</sup>Now at Dept. of Atmospheric Sciences, University of Washington, Seattle, WA, U.S.A., 98168

469 <sup>d</sup>Now at BIC-ESAT and SKL-ESPC, College of Environmental Sciences and Engineering, Peking  
470 University, Beijing 100871, China

471 <sup>e</sup>Now at NERC Centre for Ecology & Hydrology, Edinburgh, EH26 0QB, United Kingdom

472 <sup>f</sup>Now at Department of Environmental Sciences and Engineering, Gillings School of Global Public  
473 Health, University of North Carolina, Chapel Hill, North Carolina 27599, U.S.A.

474

475 ACKNOWLEDGMENT

476 L. D. Y. was supported by the UC Berkeley Chancellor's Postdoctoral Fellowship. G. I. VW.  
477 was supported by the NSF Graduate Research Fellowship (#DGE 1106400). SV-TAG data was  
478 collected by G. I. VW, L. D. Y, N. M. K., and R. A. W. as part of the SOAS and GoAmazon2014/5  
479 field campaign, funded by NSF Atmospheric Chemistry Program #1250569 and 1332998,  
480 respectively. The instrument as deployed was developed through support from U.S. Department  
481 of Energy (DOE) SBIR grant DE-SC0004698 in collaboration with S. V. H, and A. H. G. Data  
482 collection and analysis was supported in large part by NSF AGS-1243354 and the DOE Office of  
483 Science Office of Biological and Environmental Research (BER), specifically DE-SC0011105 and  
484 two user facilities: the Atmospheric Radiation Measurement (ARM) Climate Research Facility,  
485 and the Environmental Molecular Sciences Laboratory, located at Pacific Northwest National  
486 Laboratory. This publication was developed under STAR Fellowship Assistance Agreement no.  
487 FP-91778401-0 (R. A. W.) and FP-91761701-0 (B. B. P.) and awarded by the U.S. Environmental  
488 Protection Agency (EPA). It has not been formally reviewed by EPA. The views expressed in  
489 this publication are solely those of the authors, and EPA does not endorse any products or  
490 commercial services mentioned in this publication. Filter analysis by M. R. and J. D. S was  
491 supported by the U.S. EPA (#835404), NOAA Climate Program Office's AC4 Program  
492 (#NA13OAR4310064), and the Camille and Henry Dreyfus Postdoctoral Fellowship Program in  
493 Environmental Chemistry. We acknowledge the support from the Central Office of the Large  
494 Scale Biosphere Atmosphere Experiment in Amazonia (LBA), the Instituto Nacional de Pesquisas

495 da Amazonia (INPA), and the Universidade do Estado do Amazonia (UEA). P. A. acknowledges  
496 support from FAPESP through 2013/ 05014-0. The work was conducted under 001030/2012-4 of  
497 the Brazilian National Council for Scientific and Technological Development (CNPq). The CU-  
498 Boulder group was supported by DOE (BER/ASR) DE-SC0016559 and NSF AGS-1822664.

499

## 500 REFERENCES

- 501 (1) Henze, D. K.; Seinfeld, J. H. Global Secondary Organic Aerosol from Isoprene Oxidation.  
502 *Geophys. Res. Lett.* **2006**, *33* (9), L09812. <https://doi.org/10.1029/2006GL025976>.
- 503 (2) Edney, E. O.; Kleindienst, T. E.; Jaoui, M.; Lewandowski, M.; Offenberg, J. H.; Wang, W.;  
504 Claeys, M. Formation of 2-Methyl Tetrols and 2-Methylglyceric Acid in Secondary Organic  
505 Aerosol from Laboratory Irradiated Isoprene / NOX / SO2 / Air Mixtures and Their  
506 Detection in Ambient PM 2.5 Samples Collected in the Eastern United States. *Atmos.*  
507 *Environ.* **2005**, *39*, 5281–5289. <https://doi.org/10.1016/j.atmosenv.2005.05.031>.
- 508 (3) Kroll, J. H.; Ng, N. L.; Murphy, S. M.; Flagan, R. C.; Seinfeld, J. H. Secondary Organic  
509 Aerosol Formation from Isoprene Photooxidation. *Environ. Sci. Technol.* **2006**, *40* (6),  
510 1869–1877. <https://doi.org/10.1021/es0524301>.
- 511 (4) Kleindienst, T. E.; Edney, E. O.; Lewandowski, M.; Offenberg, J. H.; Jaoui, M. Secondary  
512 Organic Carbon and Aerosol Yields from the Irradiations of Isoprene and A-Pinene in the  
513 Presence of NOx and SO2. *Environ. Sci. Technol.* **2006**, *40*, 3807–3812.  
514 <https://doi.org/10.1021/es052446r>.
- 515 (5) Surratt, J. D.; Kroll, J. H.; Kleindienst, T. E.; Edney, E. O.; Claeys, M.; Sorooshian, A.; Ng,  
516 N. L.; Offenberg, J. H.; Lewandowski, M.; Jaoui, M.; Flagan, R. C.; Seinfeld, J. H. Evidence  
517 for Organosulfates in Secondary Organic Aerosol. *Environ. Sci. Technol.* **2007**, *41* (2), 517–  
518 527.
- 519 (6) Goldstein, A. H.; Koven, C. D.; Heald, C. L.; Fung, I. Y. Biogenic Carbon and  
520 Anthropogenic Pollutants Combine to Form a Cooling Haze over the Southeastern United  
521 States. *Proc. Natl. Acad. Sci. U. S. A.* **2009**, *106* (22), 8835–8840.

- 522 https://doi.org/10.1073/pnas.0904128106.
- 523 (7) Shrivastava, M. K.; Andreae, M. O.; Artaxo, P.; Barbosa, H. M. J.; Berg, L. K.; Brito, J.;  
524 Ching, J.; Easter, R. C.; Fan, J.; Fast, J. D.; Feng, Z.; Fuentes, J. D.; Glasius, M.; Goldstein,  
525 A. H.; Alves, E. G.; Gomes, H.; Gu, D.; Guenther, A.; Jathar, S. H.; Kim, S.; Liu, Y.; Lou,  
526 S.; Martin, S. T.; McNeill, V. F.; Medeiros, A.; de Sá, S. S.; Shilling, J. E.; Springston, S.  
527 R.; Souza, R. A. F.; Thornton, J. A.; Isaacman-VanWertz, G.; Yee, L. D.; Ynoue, R.; Zaveri,  
528 R. A.; Zelenyuk, A.; Zhao, C. Urban Pollution Greatly Enhances Formation of Natural  
529 Aerosols over the Amazon Rainforest. *Nat. Commun.* **2019**, *10* (1), 1046.  
530 https://doi.org/10.1038/s41467-019-10890-4.
- 531 (8) Lin, Y.-H.; Knipping, E. M.; Edgerton, E. S.; Shaw, S. L.; Surratt, J. D. Investigating the  
532 Influences of SO<sub>2</sub> and NH<sub>3</sub> Levels on Isoprene-Derived Secondary Organic Aerosol  
533 Formation Using Conditional Sampling Approaches. *Atmos. Chem. Phys.* **2013**, *13* (16),  
534 8457–8470. https://doi.org/10.5194/acp-13-8457-2013.
- 535 (9) Xu, L.; Guo, H.; Boyd, C. M.; Klein, M.; Bougiatioti, A.; Cerully, K. M.; Hite, J. R.;  
536 Isaacman-VanWertz, G.; Kreisberg, N. M.; Knote, C.; Olson, K.; Koss, A.; Goldstein, A.  
537 H.; Hering, S. V.; de Gouw, J.; Baumann, K.; Lee, S.-H.; Nenes, A.; Weber, R. J.; Ng, N. L.  
538 Effects of Anthropogenic Emissions on Aerosol Formation from Isoprene and  
539 Monoterpenes in the Southeastern United States. *Proc. Natl. Acad. Sci.* **2015**, *112* (1), 37–  
540 42. https://doi.org/10.1073/pnas.1417609112.
- 541 (10) Budisulistiorini, S. H.; Li, X.; Bairai, S. T.; Renfro, J.; Liu, Y.; Liu, Y. J.; McKinney, K. A.;  
542 Martin, S. T.; McNeill, V. F.; Pye, H. O. T.; Nenes, A.; Neff, M. E.; Stone, E. A.; Mueller,  
543 S.; Knote, C.; Shaw, S. L.; Zhang, Z.; Gold, A.; Surratt, J. D. Examining the Effects of

544 Anthropogenic Emissions on Isoprene-Derived Secondary Organic Aerosol Formation  
545 during the 2013 Southern Oxidant and Aerosol Study (SOAS) at the Look Rock, Tennessee  
546 Ground Site. *Atmos. Chem. Phys.* **2015**, *15*, 8871–8888. <https://doi.org/10.5194/acp-15-8871-2015>.

548 (11) Rattanavaraha, W.; Chu, K.; Budisulistiorini, S. H.; Riva, M.; Lin, Y.-H.; Edgerton, E. S.;  
549 Baumann, K.; Shaw, S. L.; Guo, H.; King, L.; Weber, R. J.; Neff, M. E.; Stone, E. A.;  
550 Offenberg, J. H.; Zhang, Z.; Gold, A.; Surratt, J. D. Assessing the Impact of Anthropogenic  
551 Pollution on Isoprene-Derived Secondary Organic Aerosol Formation in PM 2.5 Collected  
552 from the Birmingham, Alabama, Ground Site during the 2013 Southern Oxidant and  
553 Aerosol Study. *Atmos. Chem. Phys.* **2016**, *16* (8), 4897–4914. <https://doi.org/10.5194/acp-16-4897-2016>.

555 (12) Budisulistiorini, S. H.; Nenes, A.; Carlton, A. G.; Surratt, J. D.; McNeill, V. F.; Pye, H. O.  
556 T. Simulating Aqueous-Phase Isoprene-Epoxydiol (IEPOX) Secondary Organic Aerosol  
557 Production During the 2013 Southern Oxidant and Aerosol Study (SOAS). *Environ. Sci.  
558 Technol.* **2017**, *51* (9), 5026–5034. <https://doi.org/10.1021/acs.est.6b05750>.

559 (13) de Sá, S. S.; Palm, B. B.; Campuzano-Jost, P.; Day, D. A.; Newburn, M. K.; Hu, W.;  
560 Isaacman-VanWertz, G.; Yee, L. D.; Thalman, R.; Brito, J.; Carbone, S.; Artaxo, P.;  
561 Goldstein, A. H.; Manzi, A. O.; Souza, R. A. F.; Mei, F.; Shilling, J. E.; Springston, S. R.;  
562 Wang, J.; Surratt, J. D.; Alexander, M. L. L.; Jimenez, J. L.; Martin, S. T. Influence of  
563 Urban Pollution on the Production of Organic Particulate Matter from Isoprene Epoxydiols  
564 in Central Amazonia. *Atmos. Chem. Phys.* **2017**, *17* (11), 6611–6629.  
565 <https://doi.org/10.5194/acp-17-6611-2017>.

- 566 (14) Riva, M.; Chen, Y.; Zhang, Y.; Lei, Z.; Olson, N.; Boyer, H. C.; Narayan, S.; Yee, L. D.;  
567 Green, H.; Cui, T.; Zhang, Z.; Baumann, K. D.; Fort, M.; Edgerton, E. S.; Budisulistiorini,  
568 S.; Rose, C. A.; Ribeiro, I.; e Oliveira, R. L.; Santos, E.; Szopa, S.; Machado, C.; Zhao, Y.;  
569 Alves, E.; de Sá, S. S.; Hu, W.; Knipping, E.; Shaw, S.; Duvoisin Junior, S.; de Souza, R.  
570 A. F.; Palm, B. B.; Jimenez, J. L.; Glasius, M.; Goldstein, A.; Pye, H. O. T.; Gold, A.;  
571 Turpin, B. J.; Vizuete, W.; Martin, S. T.; Thornton, J.; Dutcher, C. S.; Ault, A. P.; Surratt,  
572 J. D. Increasing Isoprene Epoxydiol-to-Inorganic Sulfate Aerosol (IEPOX:Sulf) Ratio  
573 Results in Extensive Conversion of Inorganic Sulfate to Organosulfur Forms: Implications  
574 for Aerosol Physicochemical Properties. *Environ. Sci. Technol.* **2019**, *53* (15), 8682–8694.  
575 <https://doi.org/10.1021/acs.est.9b01019>.
- 576 (15) Surratt, J. D.; Murphy, S. M.; Kroll, J. H.; Ng, N. L.; Hildebrandt, L.; Sorooshian, A.;  
577 Szmigielski, R.; Vermeylen, R.; Maenhaut, W.; Claeys, M.; Flagan, R. C.; Seinfeld, J. H.  
578 Chemical Composition of Secondary Organic Aerosol Formed from the Photooxidation of  
579 Isoprene. *J. Phys. Chem. A* **2006**, *110* (31), 9665–9690. <https://doi.org/10.1021/jp061734m>.
- 580 (16) Wang, W.; Iinuma, Y.; Kahnt, A.; Ryabtsova, O.; Mutzel, A.; Vermeylen, R.; Van der  
581 Veken, P.; Maenhaut, W.; Herrmann, H.; Claeys, M. Formation of Secondary Organic  
582 Aerosol Marker Compounds from the Photooxidation of Isoprene and Isoprene-Derived  
583 Alkene Diols under Low-NO<sub>x</sub> Conditions. *Faraday Discuss.* **2013**, *165*, 261.  
584 <https://doi.org/10.1039/c3fd00092c>.
- 585 (17) Chan, A. W. H.; Chan, M. N.; Surratt, J. D.; Chhabra, P. S.; Loza, C. L.; Crounse, J. D.;  
586 Yee, L. D.; Flagan, R. C.; Wennberg, P. O.; Seinfeld, J. H. Role of Aldehyde Chemistry  
587 and NO<sub>x</sub> Concentrations in Secondary Organic Aerosol Formation. *Atmos. Chem. Phys.*

- 588           **2010**, *10* (15), 7169–7188. <https://doi.org/10.5194/acp-10-7169-2010>.
- 589       (18) Xu, L.; Kollman, M. S.; Song, C.; Shilling, J. E.; Ng, N. L. Effects of NO<sub>x</sub> on the Volatility  
590           of Secondary Organic Aerosol from Isoprene Photooxidation. *Environ. Sci. Technol.* **2014**,  
591           *48* (4), 2253–2262. <https://doi.org/10.1021/es404842g>.
- 592       (19) Liu, J.; D'Ambro, E. L.; Lee, B. H.; Lopez-Hilfiker, F. D.; Zaveri, R. A.; Rivera-Rios, J.  
593           C.; Keutsch, F. N.; Iyer, S.; Kurten, T.; Zhang, Z.; Gold, A.; Surratt, J. D.; Shilling, J. E.;  
594           Thornton, J. A. Efficient Isoprene Secondary Organic Aerosol Formation from a Non-  
595           IEPOX Pathway. *Environ. Sci. Technol.* **2016**, *50* (18), 9872–9880.  
596           <https://doi.org/10.1021/acs.est.6b01872>.
- 597       (20) Wennberg, P. O.; Bates, K. H.; Crounse, J. D.; Dodson, L. G.; McVay, R. C.; Mertens, L.  
598           A.; Nguyen, T. B.; Praske, E.; Schwantes, R. H.; Smarte, M. D.; St Clair, J. M.; Teng, A.  
599           P.; Zhang, X.; Seinfeld, J. H. Gas-Phase Reactions of Isoprene and Its Major Oxidation  
600           Products. *Chem. Rev.* **2018**, *118* (7), 3337–3390.  
601           <https://doi.org/10.1021/acs.chemrev.7b00439>.
- 602       (21) Surratt, J. D.; Chan, A. W. H.; Eddingsaas, N. C.; Chan, M. N.; Loza, C. L.; Kwan, A. J.;  
603           Hersey, S. P.; Flagan, R. C.; Wennberg, P. O.; Seinfeld, J. H. Reactive Intermediates  
604           Revealed in Secondary Organic Aerosol Formation from Isoprene. *Proc. Natl. Acad. Sci.  
U. S. A.* **2010**, *107* (15), 6640–6645. <https://doi.org/10.1073/pnas.0911114107>.
- 606       (22) Lin, Y.-H.; Surratt, J. D.; Zhang, Z.; Docherty, K. S.; Zhang, H.; Budisulistiorini, S. H.;  
607           Rubitschun, C. L.; Shaw, S. L.; Knipping, E. M.; Edgerton, E. S.; Kleindienst, T. E.; Gold,  
608           A. Isoprene Epoxydiols as Precursors to Secondary Organic Aerosol Formation: Acid-  
609           Catalyzed Reactive Uptake Studies with Authentic Compounds. *Environ. Sci. Technol.*

- 610           **2012**, *46* (1), 250–258. <https://doi.org/10.1021/es202554c>.
- 611       (23) Riedel, T. P.; Lin, Y.-H.; Zhang, Z.; Chu, K.; Thornton, J. A.; Vizuete, W.; Gold, A.; Surratt,  
612           J. D. Constraining Condensed-Phase Formation Kinetics of Secondary Organic Aerosol  
613           Components from Isoprene Epoxydiols. *Atmos. Chem. Phys.* **2016**, *16*, 1245–1254.  
614           <https://doi.org/10.5194/acp-16-1245-2016>.
- 615       (24) Surratt, J. D.; Lewandowski, M.; Offenberg, J. H.; Jaoui, M.; Kleindienst, T. E.; Edney, E.  
616           O.; Seinfeld, J. H. Effect of Acidity on Secondary Organic Aerosol Formation from  
617           Isoprene. *Environ. Sci. Technol.* **2007**, *41* (15), 5363–5369.  
618           <https://doi.org/10.1021/es0704176>.
- 619       (25) Woo, J. L.; McNeill, V. F. SimpleGAMMA v1.0 – a Reduced Model of Secondary Organic  
620           Aerosol Formation in the Aqueous Aerosol Phase (AaSOA). *Geosci. Model Dev.* **2015**, *8*  
621           (6), 1821–1829. <https://doi.org/10.5194/gmd-8-1821-2015>.
- 622       (26) Pye, H. O. T.; Pinder, R. W.; Piletic, I. R.; Xie, Y.; Capps, S. L.; Lin, Y.-H.; Surratt, J. D.;  
623           Zhang, Z.; Gold, A.; Luecken, D. J.; Hutzell, W. T.; Jaoui, M.; Offenberg, J. H.; Kleindienst,  
624           T. E.; Lewandowski, M.; Edney, E. O. Epoxide Pathways Improve Model Predictions of  
625           Isoprene Markers and Reveal Key Role of Acidity in Aerosol Formation. *Environ. Sci.  
626           Technol.* **2013**, *47* (19), 11056–11064. <https://doi.org/10.1021/es402106h>.
- 627       (27) Gaston, C. J.; Riedel, T. P.; Zhang, Z.; Gold, A.; Surratt, J. D.; Thornton, J. A. Reactive  
628           Uptake of an Isoprene-Derived Epoxydiol to Submicron Aerosol Particles. *Environ. Sci.  
629           Technol.* **2014**, *48*, 11178–11186. <https://doi.org/10.1021/es5034266>.
- 630       (28) Riedel, T. P.; Lin, Y.; Budisulistiorini, S. H.; Gaston, C. J.; Thornton, J. A.; Zhang, Z.;

- 631 Vizuete, W.; Gold, A.; Surratt, J. D. Heterogeneous Reactions of Isoprene-Derived  
632 Epoxides: Reaction Probabilities and Molar Secondary Organic Aerosol Yield Estimates.  
633 *Environ. Sci. Technol. Lett.* **2015**, *2*, 38–42. <https://doi.org/10.1021/ez500406f>.
- 634 (29) Marais, E. A.; Jacob, D. J.; Jimenez, J. L.; Campuzano-Jost, P.; Day, D. A.; Hu, W. W.;  
635 Krechmer, J. E.; Zhu, L.; Kim, P. S.; Miller, C. C.; Fisher, J. A.; Travis, K.; Yu, K.; Hanisco,  
636 T. F.; Wolfe, G. M.; Arkinson, H. L.; Pye, H. O. T.; Froyd, K. D.; Liao, J.; McNeill, V. F.  
637 Aqueous-Phase Mechanism for Secondary Organic Aerosol Formation from Isoprene :  
638 Application to the Southeast United States and Co-Benefit of SO<sub>2</sub> Emission Controls.  
639 *Atmos. Chem. Phys.* **2016**, *16*, 1603–1618. <https://doi.org/10.5194/acp-16-1603-2016>.
- 640 (30) Paulot, F.; Crounse, J. D.; Kjaergaard, H. G.; Kürten, A.; St Clair, J. M.; Seinfeld, J. H.;  
641 Wennberg, P. O. Unexpected Epoxide Formation in the Gas-Phase Photooxidation of  
642 Isoprene. *Science* **2009**, *325* (5941), 730–733. <https://doi.org/10.1126/science.1172910>.
- 643 (31) Liu, Y. J.; Kuwata, M.; Strick, B. F.; Geiger, F. M.; Thomson, R. J.; McKinney, K. a.;  
644 Martin, S. T. Uptake of Epoxydiol Isomers Accounts for Half of the Particle-Phase Material  
645 Produced from Isoprene Photooxidation via the HO<sub>2</sub> Pathway. *Environ. Sci. Technol.* **2015**,  
646 *49* (1), 250–258. <https://doi.org/10.1021/es5034298>.
- 647 (32) Bates, K. H.; Crounse, J. D.; St. Clair, J. M.; Bennett, N. B.; Nguyen, T. B.; Seinfeld, J. H.;  
648 Stoltz, B. M.; Wennberg, P. O. Gas Phase Production and Loss of Isoprene Epoxydiols. *J.  
649 Phys. Chem. A* **2014**, *118* (7), 1237–1246. <https://doi.org/10.1021/jp4107958>.
- 650 (33) Nguyen, T. B.; Coggon, M. M.; Bates, K. H.; Zhang, X.; Schwantes, R. H.; Schilling, K.  
651 A.; Loza, C. L.; Flagan, R. C.; Wennberg, P. O.; Seinfeld, J. H. Organic Aerosol Formation  
652 from the Reactive Uptake of Isoprene Epoxydiols (IEPOX) onto Non-Acidified Inorganic

- 653 Seeds. *Atmos. Chem. Phys.* **2014**, *14* (7), 3497–3510. <https://doi.org/10.5194/acp-14-3497-2014>.
- 654
- 655 (34) Budisulistiorini, S. H.; Canagaratna, M. R.; Croteau, P. L.; Marth, W. J.; Baumann, K.;  
656 Edgerton, E. S.; Shaw, S. L.; Knipping, E. M.; Worsnop, D. R.; Jayne, J. T.; Gold, A.;  
657 Surratt, J. D. Real-Time Continuous Characterization of Secondary Organic Aerosol  
658 Derived from Isoprene Epoxydiols in Downtown Atlanta, Georgia, Using the Aerodyne  
659 Aerosol Chemical Speciation Monitor. *Environ. Sci. Technol.* **2013**, *47* (11), 5686–5694.  
660 <https://doi.org/10.1021/es400023n>.
- 661 (35) Claeys, M.; Graham, B.; Vas, G.; Wang, W.; Vermeylen, R.; Pashynska, V.; Cafmeyer, J.;  
662 Guyon, P.; Andreae, M. O.; Artaxo, P.; Maenhaut, W. Formation of Secondary Organic  
663 Aerosols through Photooxidation of Isoprene. *Science* **2004**, *303* (5661), 1173–1176.  
664 <https://doi.org/10.1126/science.1092805>.
- 665 (36) Claeys, M.; Kourtchev, I.; Pashynska, V.; Vas, G.; Vermeylen, R.; Wang, W.; Cafmeyer,  
666 J.; Chi, X.; Artaxo, P.; Andreae, M. O.; Maenhaut, W. Polar Organic Marker Compounds  
667 in Atmospheric Aerosols during the LBA-SMOCC 2002 Biomass Burning Experiment in  
668 Rondônia, Brazil: Sources and Source Processes, Time Series, Diel Variations and Size  
669 Distributions. *Atmos. Chem. Phys.* **2010**, *10*, 9319–9331. <https://doi.org/10.5194/acp-10-9319-2010>.
- 670
- 671 (37) Lin, Y.; Budisulistiorini, S. H.; Chu, K.; Siejack, R. A.; Zhang, H.; Riva, M.; Zhang, Z.;  
672 Gold, A.; Kautzman, K. E.; Surratt, J. D. Light-Absorbing Oligomer Formation in  
673 Secondary Organic Aerosol from Reactive Uptake of Isoprene Epoxydiols. *Environ. Sci.  
674 Technol.* **2014**, *48* (20), 12012–12021. <https://doi.org/10.1021/es503142b>.

- 675 (38) Wang, W.; Kourtchev, I.; Graham, B.; Cafmeyer, J.; Maenhaut, W.; Claeys, M.  
676 Characterization of Oxygenated Derivatives of Isoprene Related to 2-Methyltetrosols in  
677 Amazonian Aerosols Using Trimethylsilylation and Gas Chromatography/Ion Trap Mass  
678 Spectrometry. *Rapid Commun. Mass Spectrom.* **2005**, *19* (10), 1343–1351.  
679 <https://doi.org/10.1002/rcm.1940>.
- 680 (39) Kleindienst, T. E.; Lewandowski, M.; Offenberg, J. H.; Jaoui, M.; Edney, E. O. The  
681 Formation of Secondary Organic Aerosol from the Isoprene + OH Reaction in the Absence  
682 of NO<sub>x</sub>. *Atmos. Chem. Phys.* **2009**, *9* (17), 6541–6558. <https://doi.org/10.5194/acp-9-6541-2009>.
- 684 (40) Froyd, K. D.; Murphy, S. M.; Murphy, D. M.; Gouw, J. A. de; Eddingsaas, N. C.; Wennberg,  
685 P. O. Contribution of Isoprene-Derived Organosulfates to Free Tropospheric Aerosol Mass.  
686 *Proc. Natl. Acad. Sci.* **2010**, *107* (50), 21360–21365.  
687 <https://doi.org/10.1073/PNAS.1012561107>.
- 688 (41) Pratt, K. a.; Fiddler, M. N.; Shepson, P. B.; Carlton, A. G.; Surratt, J. D. Organosulfates in  
689 Cloud Water above the Ozarks' Isoprene Source Region. *Atmos. Environ.* **2013**, *77*, 231–  
690 238. <https://doi.org/10.1016/j.atmosenv.2013.05.011>.
- 691 (42) Cui, T.; Zeng, Z.; dos Santos, E. O.; Zhang, Z.; Chen, Y.; Zhang, Y.; Rose, C. A.;  
692 Budisulistiorini, S. H.; Collins, L. B.; Bodnar, W. M.; de Souza, R. A. F.; Martin, S. T.;  
693 Machado, C. M. D.; Turpin, B. J.; Gold, A.; Ault, A. P.; Surratt, J. D. Development of a  
694 Hydrophilic Interaction Liquid Chromatography (HILIC) Method for the Chemical  
695 Characterization of Water-Soluble Isoprene Epoxydiol (IEPOX)-Derived Secondary  
696 Organic Aerosol. *Environ. Sci. Process. Impacts* **2018**, *20*, 1524–1536.

- 697 https://doi.org/10.1039/c8em00308d.
- 698 (43) Isaacman-VanWertz, G.; Yee, L. D.; Kreisberg, N. M.; Wernis, R.; Moss, J. A.; Hering, S.  
699 V.; de Sá, S. S.; Martin, S. T.; Alexander, M. L.; Palm, B. B.; Hu, W. W.; Campuzano-Jost,  
700 P.; Day, D. A.; Jimenez, J. L.; Riva, M.; Surratt, J. D.; Viegas, J.; Manzi, A.; Edgerton, E.  
701 S.; Baumann, K.; Souza, R.; Artaxo, P.; Goldstein, A. H. Ambient Gas-Particle Partitioning  
702 of Tracers for Biogenic Oxidation. *Environ. Sci. Technol.* **2016**, *50* (18), 9952–9962.  
703 https://doi.org/10.1021/acs.est.6b01674.
- 704 (44) Lopez-Hilfiker, F. D.; Mohr, C.; D'Ambro, E. L.; Lutz, A.; Riedel, T. P.; Gaston, C. J.; Iyer,  
705 S.; Zhang, Z.; Gold, A.; Surratt, J. D.; Lee, B. H.; Kurten, T.; Hu, W. W.; Jimenez, J.;  
706 Hallquist, M.; Thornton, J. A. Molecular Composition and Volatility of Organic Aerosol in  
707 the Southeastern U. S.: Implications for IEPOX Derived SOA. *Environ. Sci. Technol.* **2016**,  
708 *50*, 2200–2209. https://doi.org/10.1021/acs.est.5b04769.
- 709 (45) Hu, W.; Palm, B. B.; Day, D. A.; Campuzano-Jost, P.; Krechmer, J. E.; Peng, Z.; de Sá, S.  
710 S.; Martin, S. T.; Alexander, M. L.; Baumann, K.; Hacker, L.; Kiendler-Scharr, A.; Koss,  
711 A. R.; De Gouw, J. A.; Goldstein, A. H.; Seco, R.; Sjostedt, S. J.; Park, J.-H.; Guenther, A.  
712 B.; Kim, S.; Canonaco, F.; Prévôt, A. S. H.; Brune, W. H.; Jimenez, J. L. Volatility and  
713 Lifetime against OH Heterogeneous Reaction of Ambient Isoprene-Epoxydiols-Derived  
714 Secondary Organic Aerosol (IEPOX-SOA). *Atmos. Chem. Phys.* **2016**, *16*, 11563–11580.  
715 https://doi.org/10.5194/acp-16-11563-2016.
- 716 (46) Kroll, J. H.; Ng, N. L.; Murphy, S. M.; Flagan, R. C.; Seinfeld, J. H. Secondary Organic  
717 Aerosol Formation from Isoprene Photooxidation under High-NO<sub>x</sub> Conditions. *Geophys.  
718 Res. Lett.* **2005**, *32* (18), 1–4. https://doi.org/10.1029/2005GL023637.

- 719 (47) Lin, Y.-H.; Zhang, H.; Pye, H. O. T.; Zhang, Z.; Marth, W. J.; Park, S.; Arashiro, M.; Cui,  
720 T.; Budisulistiorini, S. H.; Sexton, K. G.; Vizuete, W.; Xie, Y.; Luecken, D. J.; Piletic, I.  
721 R.; Edney, E. O.; Bartolotti, L. J.; Gold, A.; Surratt, J. D. Epoxide as a Precursor to  
722 Secondary Organic Aerosol Formation from Isoprene Photooxidation in the Presence of  
723 Nitrogen Oxides. *Proc. Natl. Acad. Sci. U. S. A.* **2013**, *110* (17), 6718–6723.  
724 <https://doi.org/10.1073/pnas.1221150110>.
- 725 (48) Nguyen, T. B.; Bates, K. H.; Crounse, J. D.; Schwantes, R. H.; Zhang, X.; Kjaergaard, H.  
726 G.; Surratt, J. D.; Lin, P.; Laskin, A.; Seinfeld, J. H.; Wennberg, P. O. Mechanism of the  
727 Hydroxyl Radical Oxidation of Methacryloyl Peroxynitrate (MPAN) and Its Pathway  
728 toward Secondary Organic Aerosol Formation in the Atmosphere. *Phys. Chem. Chem. Phys.*  
729 **2015**, *17*, 17914–17926. <https://doi.org/10.1039/C5CP02001H>.
- 730 (49) Dommen, J.; Metzger, A.; Duplissy, J.; Kalberer, M.; Alfarra, M. R.; Gascho, A.;  
731 Weingartner, E.; Prevot, A. S. H.; Verheggen, B.; Baltensperger, U. Laboratory Observation  
732 of Oligomers in the Aerosol from Isoprene/NO<sub>x</sub> Photooxidation. *Geophys. Res. Lett.* **2006**,  
733 *33* (13), L13805. <https://doi.org/10.1029/2006GL026523>.
- 734 (50) Szmigielski, R.; Surratt, J. D.; Vermeylen, R.; Szmigielska, K.; Kroll, J. H.; Ng, N. L.;  
735 Murphy, S. M.; Sorooshian, A.; Seinfeld, J. H.; Claeys, M. Characterization of 2-  
736 Methylglyceric Acid Oligomers in Secondary Organic Aerosol Formed from the  
737 Photooxidation of Isoprene Using Trimethylsilylation and Gas Chromatography/Ion Trap  
738 Mass Spectrometry. *J. Mass Spectrom.* **2007**, *42* (1), 101–116.  
739 <https://doi.org/10.1002/jms.1146>.
- 740 (51) Worton, D. R.; Surratt, J. D.; LaFranchi, B. W.; Chan, A. W. H.; Zhao, Y.; Weber, R. J.;

- 741 Park, J.-H.; Gilman, J. B.; De Gouw, J.; Park, C.; Schade, G.; Beaver, M. R.; St. Clair, J.  
742 M.; Crounse, J. D.; Wennberg, P. O.; Wolfe, G. M.; Harrold, S.; Thornton, J. A.; Farmer,  
743 D.; Docherty, K. S.; Cubison, M.; Jimenez, J. L.; Frossard, A. A.; Russell, L. M.; Kristensen,  
744 K.; Glasius, M.; Mao, J.; Ren, X.; Brune, B.; Browne, E. C.; Pusede, S.; Cohen, R. C.;  
745 Seinfeld, J. H.; Goldstein, A. H. Observational Insights into Aerosol Formation from  
746 Isoprene. *Environ. Sci. Technol.* **2013**, *47* (20), 11403–11413.  
747 <https://doi.org/10.1021/es4011064>.
- 748 (52) Carlton, A. G.; de Gouw, J.; Jimenez, J. L.; Ambrose, J. L.; Attwood, A. R.; Brown, S.;  
749 Baker, K. R.; Brock, C.; Cohen, R. C.; Edgerton, S.; Farkas, C. M.; Farmer, D.; Goldstein,  
750 A. H.; Gratz, L.; Guenther, A.; Hunt, S.; Jaeglé, L.; Jaffe, D. A.; Mak, J.; McClure, C.;  
751 Nenes, A.; Nguyen, T. K.; Pierce, J. R.; de Sá, S. S.; Selin, N. E.; Shah, V.; Shaw, S.;  
752 Shepson, P. B.; Stutz, J.; Surratt, J. D.; Turpin, B. J.; Warneke, C.; Washenfelder, R. A.;  
753 Wennberg, P. O.; Zhou, X. Synthesis of the Southeast Atmosphere Studies. *Bull. Am.  
754 Meteorological Soc.* **2018**, 547–567. <https://doi.org/10.1175/BAMS-D-16-0048.1>.
- 755 (53) Martin, S. T.; Artaxo, P.; Machado, L. A. T.; Manzi, A. O.; Souza, R. A. F.; Schumacher,  
756 C.; Wang, J.; Andreae, M. O.; Barbosa, H. M. J.; Fan, J.; Fisch, G.; Goldstein, A. H.;  
757 Guenther, A. B.; Jimenez, J. L.; Pöschl, U.; Silva Dias, M. A.; Smith, J. N.; Wendisch, M.  
758 Introduction: Observations and Modeling of the Green Ocean Amazon (GoAmazon2014/5).  
759 *Atmos. Chem. Phys.* **2016**, *16* (8), 4785–4797. <https://doi.org/10.5194/acp-16-4785-2016>.
- 760 (54) Martin, S. T.; Artaxo, P.; Machado, L. A. T.; Manzi, A. O.; Souza, R. A. F.; Schumacher,  
761 C.; Wang, J.; Biscaro, T.; Brito, J.; Calheiros, A.; Jardine, K. J.; Medeiros, A.; Portela, B.;  
762 de Sá, S. S.; Adachi, K.; Aiken, A. C.; Albrecht, R.; Alexander, L.; Andreae, M. O.;

- 763 Barbosa, H. M. J.; Buseck, P.; Chand, D.; Comstock, J. M.; Day, D. A.; Dubey, M.; Fan, J.;  
764 Fast, J.; Fisch, G.; Fortner, E.; Giangrande, S.; Gilles, M.; Goldstein, A. H.; Guenther, A.;  
765 Hubbe, J.; Jensen, M.; Jimenez, J. L.; Keutsch, F. N.; Kim, S.; Kuang, C.; Laskin, A.;  
766 McKinney, K.; Mei, F.; Miller, M.; Nascimento, R.; Pauliquevis, T.; Pekour, M.; Peres, J.;  
767 Petäjä, T.; Pöhlker, C.; Pöschl, U.; Rizzo, L.; Schmid, B.; Shilling, J. E.; Dias, M. A. S.;  
768 Smith, J. N.; Tomlinson, J. M.; Tóta, J.; Wendisch, M. The Green Ocean Amazon  
769 Experiment (GoAmazon2014/5) Observes Pollution Affecting Gases, Aerosols, Clouds,  
770 and Rainfall over the Rain Forest. *Bull. Am. Meteorol. Soc.* **2017**, *98* (5), 981–997.  
771 <https://doi.org/10.1175/BAMS-D-15-00221.1>.
- 772 (55) de Sá, S. S.; Rizzo, L. V.; Palm, B. B.; Campuzano-Jost, P.; Day, D. A.; Yee, L. D.; Wernis,  
773 R.; Isaacman-VanWertz, G.; Brito, J.; Carbone, S.; Liu, Y. J.; Sedlacek, A.; Springston, S.;  
774 Goldstein, A. H.; Barbosa, H. M. J.; Alexander, M. L.; Artaxo, P.; Jimenez, J. L.; Martin,  
775 S. T. Contributions of Biomass-Burning, Urban, and Biogenic Emissions to the  
776 Concentrations and Light-Absorbing Properties of Particulate Matter in Central Amazonia  
777 during the Dry Season. *Atmos. Chem. Phys.* **2019**, *19* (12), 7973–8001.  
778 <https://doi.org/10.5194/acp-19-7973-2019>.
- 779 (56) Isaacman, G. A.; Kreisberg, N. M.; Yee, L. D.; Worton, D. R.; Chan, A. W. H.; Moss, J.  
780 A.; Hering, S. V.; Goldstein, A. H. Online Derivatization for Hourly Measurements of Gas-  
781 and Particle-Phase Semi-Volatile Oxygenated Organic Compounds by Thermal Desorption  
782 Aerosol Gas Chromatography (SV-TAG). *Atmos. Meas. Tech.* **2014**, *7* (12), 4417–4429.  
783 <https://doi.org/10.5194/amt-7-4417-2014>.
- 784 (57) Yee, L. D.; Isaacman-Vanwertz, G.; Wernis, R. A.; Meng, M.; Rivera, V.; Kreisberg, N.

- 785 M.; Hering, S. V.; Bering, M. S.; Glasius, M.; Upshur, M. A.; Bé, A. G.; Thomson, R. J.;  
786 Geiger, F. M.; Offenberg, J. H.; Lewandowski, M.; Kourtchev, I.; Kalberer, M.; de Sá, S.  
787 S.; Martin, S. T.; Alexander, M. L.; Palm, B. B.; Hu, W.; Campuzano-Jost, P.; Day, D. A.;  
788 Jimenez, J. L.; Liu, Y. J.; McKinney, K. A.; Artaxo, P.; Viegas, J.; Manzi, A.; Oliveira, M.  
789 B.; De Souza, R.; Machado, L. A. T.; Longo, K.; Goldstein, A. H. Observations of  
790 Sesquiterpenes and Their Oxidation Products in Central Amazonia during the Wet and Dry  
791 Seasons. *Atmos. Chem. Phys.* **2018**, *18*, 10433–10457. <https://doi.org/10.5194/acp-18-10433-2018>.
- 793 (58) Hu, W. W.; Campuzano-Jost, P.; Palm, B. B.; Day, D. A.; Ortega, A. M.; Hayes, P. L.;  
794 Krechmer, J. E.; Chen, Q.; Kuwata, M.; Liu, Y. J.; de Sá, S. S.; McKinney, K. A.; Martin,  
795 S. T.; Hu, M.; Budisulistiorini, S. H.; Riva, M.; Surratt, J. D.; St. Clair, J. M.; Isaacman-  
796 VanWertz, G.; Yee, L. D.; Goldstein, A. H.; Carbone, S.; Brito, J.; Artaxo, P.; De Gouw, J.  
797 A.; Koss, A.; Wisthaler, A.; Mikoviny, T.; Karl, T.; Kaser, L.; Jud, W.; Hansel, A.;  
798 Docherty, K. S.; Alexander, M. L.; Robinson, N. H.; Coe, H.; Allan, J. D.; Canagaratna, M.  
799 R.; Paulot, F.; Jimenez, J. L. Characterization of a Real-Time Tracer for Isoprene  
800 Epoxydiols-Derived Secondary Organic Aerosol (IEPOX-SOA) from Aerosol Mass  
801 Spectrometer Measurements. *Atmos. Chem. Phys.* **2015**, *15* (20), 11807–11833.  
802 <https://doi.org/10.5194/acp-15-11807-2015>.
- 803 (59) de Sá, S. S.; Palm, B. B.; Campuzano-Jost, P.; Day, D. A.; Hu, W.; Isaacman-VanWertz,  
804 G.; Yee, L. D.; Brito, J.; Carbone, S.; Ribeiro, I. O.; Cirino, G. G. G.; Liu, Y. J.; Thalman,  
805 R.; Sedlacek, A.; Funk, A.; Schumacher, C.; Shilling, J. E.; Schneider, J.; Artaxo, P.;  
806 Goldstein, A. H.; Souza, R. A. F.; Wang, J.; McKinney, K. A.; Barbosa, H.; Lizabeth  
807 Alexander, M.; Jimenez, J. L.; Martin, S. T. Urban Influence on the Concentration and

- 808       Composition of Submicron Particulate Matter in Central Amazonia. *Atmos. Chem. Phys.*  
809       2018, 18 (16), 1–56. <https://doi.org/10.5194/acp-18-12185-2018>.
- 810       (60) Riva, M.; Budisulistiorini, S. H.; Zhang, Z.; Gold, A.; Surratt, J. D. Chemical  
811       Characterization of Secondary Organic Aerosol Constituents from Isoprene Ozonolysis in  
812       the Presence of Acidic Aerosol. *Atmos. Environ.* 2016, 130, 5–13.  
813       <https://doi.org/10.1016/j.atmosenv.2015.06.027>.
- 814       (61) Glasius, M.; Bering, M. S.; Yee, L. D.; De Sá, S. S.; Isaacman-Vanwertz, G.; Wernis, R.  
815       A.; Barbosa, H. M. J.; Alexander, M. L.; Palm, B. B.; Hu, W.; Campuzano-Jost, P.; Day, D.  
816       A.; Jimenez, J. L.; Shrivastava, M. K.; Martin, S. T.; Goldstein, A. H. Organosulfates in  
817       Aerosols Downwind of an Urban Region in Central Amazon. *Environ. Sci. Process. Impacts*  
818       2018, 20 (11), 1546–1558. <https://doi.org/10.1039/c8em00413g>.
- 819       (62) Su, L.; Patton, E. G.; Vilà-Guerau De Arellano, J.; Guenther, A. B.; Kaser, L.; Yuan, B.;  
820       Xiong, F.; Shepson, P. B.; Zhang, L.; Miller, D. O.; Brune, W. H.; Baumann, K.; Edgerton,  
821       E.; Weinheimer, A.; Misztal, P. K.; Park, J.-H.; Goldstein, A. H.; Skog, K. M.; Keutsch, F.  
822       N.; Mak, J. E. Understanding Isoprene Photooxidation Using Observations and Modeling  
823       over a Subtropical Forest in the Southeastern US. *Atmos. Chem. Phys* 2016, 16, 7725–7741.  
824       <https://doi.org/10.5194/acp-16-7725-2016>.
- 825       (63) Liu, Y. J.; Brito, J.; Dorris, M. R.; Rivera-Rios, J. C.; Seco, R.; Bates, K. H.; Artaxo, P.;  
826       Duvoisin, S.; Keutsch, F. N.; Kim, S.; Goldstein, A. H.; Guenther, A. B.; Manzi, A. O.;  
827       Souza, R. A. F.; Springston, S. R.; Watson, T. B.; McKinney, K. A.; Martin, S. T. Isoprene  
828       Photochemistry over the Amazon Rainforest. *Proc. Natl. Acad. Sci.* 2016, 113 (22), 6125–  
829       6130. <https://doi.org/10.1073/pnas.1524136113>.

- 830 (64) Fountoukis, C.; Nenes, A. *Atmospheric Chemistry and Physics ISORROPIA II: A*  
831 *Computationally Efficient Thermodynamic Equilibrium Model for K<sup>+</sup>-Ca<sup>2+</sup>-Mg<sup>2+</sup>-NH<sub>4</sub><sup>+</sup>-Na<sup>+</sup>-SO<sub>4</sub><sup>2-</sup>-NO<sub>3</sub><sup>-</sup>-Cl<sup>-</sup>-H<sub>2</sub>O Aerosols*; 2007; Vol. 7.
- 832
- 833 (65) Hansen, D. A.; Edgerton, E. S.; Hartsell, B. E.; Jansen, J. J.; Kandasamy, N.; Hidy, G. M.;  
834 Blanchard, C. L. The Southeastern Aerosol Research and Characterization Study: Part 1-  
835 Overview. *J. Air Waste Manage. Assoc.* **2003**, *53*, 1460–1471.  
836 <https://doi.org/10.1080/10473289.2003.10466318>.
- 837 (66) Mather, J. H.; Voyles, J. W. The Arm Climate Research Facility: A Review of Structure  
838 and Capabilities. *Bull. Am. Meteorol. Soc.* **2013**, *94* (3), 377–392.  
839 <https://doi.org/10.1175/BAMS-D-11-00218.1>.
- 840 (67) Liu, Y. J.; Seco, R.; Kim, S.; Guenther, A. B.; Goldstein, A. H.; Keutsch, F. N.; Springston,  
841 S. R.; Watson, T. B.; Artaxo, P.; Souza, R. A. F.; McKinney, K. A.; Martin, S. T. Isoprene  
842 Photo-Oxidation Products Quantify the Effect of Pollution on Hydroxyl Radicals over  
843 Amazonia. *Sci. Adv.* **2018**, *4* (4), eaar2547. <https://doi.org/10.1126/sciadv.aar2547>.
- 844 (68) Hidy, G. M.; Blanchard, C. L.; Baumann, K.; Edgerton, E.; Tanenbaum, S.; Shaw, S.;  
845 Knipping, E.; Tombach, I.; Jansen, J.; Walters, J. Chemical Climatology of the Southeastern  
846 United States. *Atmos. Chem. Phys.* **2014**, *14*, 1999–2013. <https://doi.org/10.5194/acp-14-11893-2014>.
- 847
- 848 (69) Xu, L.; Middlebrook, A. M.; Liao, J.; de Gouw, J. A.; Guo, H.; Weber, R. J.; Nenes, A.;  
849 Lopez-Hilfiker, F. D.; Lee, B. H.; Thornton, J. A.; Brock, C. A.; Neuman, J. A.; Nowak, J.  
850 B.; Pollack, I. B.; Welti, A.; Graus, M.; Warneke, C.; Ng, N. L. Enhanced Formation of  
851 Isoprene-Derived Organic Aerosol in Sulfur-Rich Power Plant Plumes during Southeast

- 852            Nexus. *J. Geophys. Res. Atmos.* **2016**, *121* (18), 11,137–11,153.  
853            <https://doi.org/10.1002/2016JD025156>.
- 854        (70) Eddingsaas, N. C.; VanderVelde, D. G.; Wennberg, P. O. Kinetics and Products of the Acid-  
855            Catalyzed Ring-Opening of Atmospherically Relevant Butyl Epoxy Alcohols. *J. Phys.*  
856            *Chem. A* **2010**, *114* (31), 8106–8113. <https://doi.org/10.1021/jp103907c>.
- 857        (71) Riva, M.; Bell, D. M.; Hansen, A.-M. K.; Drozd, G. T.; Zhang, Z.; Gold, A.; Imre, D.;  
858            Surratt, J. D.; Glasius, M.; Zelenyuk, A. Effect of Organic Coatings, Humidity and Aerosol  
859            Acidity on Multiphase Chemistry of Isoprene Epoxydiols. *Environ. Sci. Technol.* **2016**, *50*  
860            (11), 5580–5588. <https://doi.org/10.1021/acs.est.5b06050>.
- 861        (72) Li, J.; Wang, G.; Wu, C.; Cao, C.; Ren, Y.; Wang, J.; Li, J.; Cao, J.; Zeng, L.; Zhu, T.  
862            Characterization of Isoprene-Derived Secondary Organic Aerosols at a Rural Site in North  
863            China Plain with Implications for Anthropogenic Pollution Effects. *Nature* **2018**, *553*,  
864            1–10. <https://doi.org/10.1038/s41598-017-18983-7>.
- 865        (73) Andreae, M. O.; Berresheim, H.; Bingemer, H.; Jacob, D. J.; Lewis, B. L.; Li, S.-M.; Talbot,  
866            R. W. The Atmospheric Sulfur Cycle over the Amazon Basin: 2. Wet Season. *J. Geophys.*  
867            *Res.* **1990**, *95* (D10), 16813. <https://doi.org/10.1029/JD095iD10p16813>.
- 868        (74) Chen, Q.; Farmer, D. K.; Schneider, J.; Zorn, S. R.; Heald, C. L.; Karl, T. G.; Guenther, A.  
869            B.; Allan, J. D.; Robinson, N. H.; Coe, H.; Kimmel, J. R.; Pauliquevis, T.; Borrmann, S.;  
870            Pöschl, U.; Andreae, M. O.; Artaxo, P.; Jimenez, J. L.; Martin, S. T. Mass Spectral  
871            Characterization of Submicron Biogenic Organic Particles in the Amazon Basin. *Geophys.*  
872            *Res. Lett.* **2009**, *36* (20), L20806. <https://doi.org/10.1029/2009GL039880>.

- 873 (75) Martin, S. T.; Andreae, M. O.; Artaxo, P.; Baumgardner, D.; Chen, Q.; Goldstein, A. H.;  
874 Guenther, A. B.; Heald, C. L.; Mayol-Bracero, O. L.; McMurry, P. H.; Pauliquevis, T.;  
875 Pöschl, U.; Prather, K. A.; Roberts, G. C.; Saleska, S. R.; Silva Dias, M. A.; Spracklen, D.  
876 V.; Swietlicki, E.; Trebs, I. Sources and Properties of Amazonian Aerosol Particles. *Rev.*  
877 *Geophys.* **2010**, *48* (2), RG2002. <https://doi.org/10.1029/2008RG000280>.
- 878 (76) Tolocka, M. P.; Turpin, B. Contribution of Organosulfur Compounds to Organic Aerosol  
879 Mass. *Environ. Sci. Technol.* **2012**, *46*, 7978–7983. <https://doi.org/10.1021/es300651v>.
- 880 (77) Hansen, A.-M. K.; Kristensen, K.; Nguyen, Q. T.; Zare, a.; Cozzi, F.; Nøjgaard, J. K.; Skov,  
881 H.; Brandt, J.; Christensen, J. H.; Ström, J.; Tunved, P.; Krejci, R.; Glasius, M.  
882 Organosulfates and Organic Acids in Arctic Aerosols: Speciation, Annual Variation and  
883 Concentration Levels. *Atmos. Chem. Phys.* **2014**, *14* (15), 7807–7823.  
884 <https://doi.org/10.5194/acp-14-7807-2014>.
- 885 (78) Kourtchev, I.; Doussin, J.-F.; Giorio, C.; Mahon, B.; Wilson, E. M.; Maurin, N.; Pangui, E.;  
886 Venables, D. S.; Wenger, J. C.; Kalberer, M. Molecular Composition of Fresh and Aged  
887 Secondary Organic Aerosol from a Mixture of Biogenic Volatile Compounds: A High-  
888 Resolution Mass Spectrometry Study. *Atmos. Chem. Phys.* **2015**, *15* (10), 5683–5695.  
889 <https://doi.org/10.5194/acp-15-5683-2015>.
- 890 (79) Kjaergaard, H. G.; Knap, H. C.; Ørnsø, K. B.; Jørgensen, S.; Crounse, J. D.; Paulot, F.;  
891 Wennberg, P. O. Atmospheric Fate of Methacrolein. 2. Formation of Lactone and  
892 Implications for Organic Aerosol Production. *J. Phys. Chem. A* **2012**, *116* (24), 5763–5768.  
893 <https://doi.org/10.1021/jp210853h>.
- 894 (80) Kuwata, M.; Liu, Y.; McKinney, K.; Martin, S. T. Physical State and Acidity of Inorganic

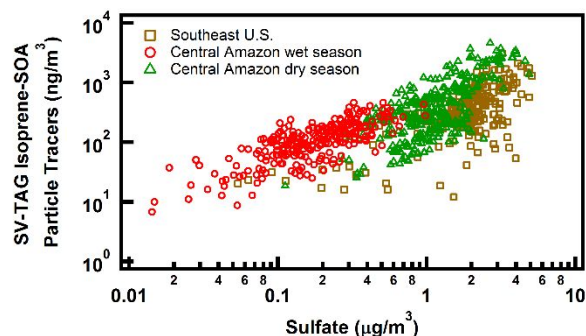
- 895 Sulfate Can Regulate the Production of Secondary Organic Material from Isoprene  
896 Photooxidation Products. *Phys. Chem. Chem. Phys.* **2015**, *17*, 5670.  
897 <https://doi.org/10.1039/c4cp04942j>.
- 900 (81) Blanchard, C. L.; Hidy, G. M.; Shaw, S.; Baumann, K.; Edgerton, E. S. Effects of Emission  
901 Reductions on Organic Aerosol in the Southeastern United States. *Atmos. Chem. Phys.*  
902 **2016**, *16*, 215–238. <https://doi.org/10.5194/acp-16-215-2016>.
- 903 (82) Jardine, K. J.; Yañez-Serrano, A. M.; Williams, J.; Kunert, N.; Jardine, A. B.; Taylor, T.;  
904 Abrell, L.; Artaxo, P.; Guenther, A.; Hewitt, C. N.; House, E.; Florentino, A. P.; Manzi, A.;  
905 Higuchi, N.; Kesselmeier, J.; Behrendt, T.; Veres, P. R.; Derstroff, B.; Fuentes, J. D.;  
906 Martin, S. T.; Andreae, M. O. Dimethyl Sulfide in the Amazon Rain Forest. *Global  
Biogeochem. Cycles* **2015**, *29*, 19–32. <https://doi.org/10.1002/2014GB004969>.
- 907 (83) Saturno, J.; Ditas, F.; Penning De Vries, M.; Holanda, B. A.; Pöhlker, M. L.; Carbone, S.;  
908 Walter, D.; Bobrowski, N.; Brito, J.; Chi, X.; Gutmann, A.; Hrabe De Angelis, I.; Machado,  
909 L. A. T.; Moran-Zuloaga, D.; Rüdiger, J.; Schneider, J.; Schulz, C.; Wang, Q.; Wendisch,  
910 M.; Artaxo, P.; Wagner, T.; Pöschl, U.; Andreae, M. O.; Pöhlker, C. African Volcanic  
911 Emissions Influencing Atmospheric Aerosols over the Amazon Rain Forest. *Atmos. Chem.  
Phys.* **2018**, *18*, 10391–10405. <https://doi.org/10.5194/acp-18-10391-2018>.
- 912 (84) Andreae, M. O.; Merlet, P. Emission of Trace Gases and Aerosols from Biomass Burning.  
913 *Global Biogeochem. Cycles* **2001**, *15* (4), 955–966.  
914 <https://doi.org/10.1029/2000GB001382>.
- 915 (85) Hand, J. L.; Schichtel, B. A.; Malm, W. C.; Pitchford, M. L. Particulate Sulfate Ion  
916 Concentration and SO<sub>2</sub> Emission Trends in the United States from the Early 1990s through

- 917 2010. *Atmos. Chem. Phys.* **2012**, *12* (21), 10353–10365. <https://doi.org/10.5194/acp-12-10353-2012>.
- 918
- 919 (86) Estillore, A. D.; Hettiyadura, A. P. S.; Qin, Z.; Leckrone, E.; Wombacher, B.; Humphry, T.;  
920 Stone, E. A.; Grassian, V. H. Water Uptake and Hygroscopic Growth of Organosulfate  
921 Aerosol. *Environ. Sci. Technol.* **2016**, *50* (8), 4259–4268.  
922 <https://doi.org/10.1021/acs.est.5b05014>.
- 923 (87) Vogel, A. L.; Schneider, J.; Müller-Tautges, C.; Phillips, G. J.; Pöhlker, M. L.; Rose, D.;  
924 Zuth, C.; Makkonen, U.; Hakola, H.; Crowley, J. N.; Andreae, M. O.; Pöschl, U.; Hoffmann,  
925 T. Aerosol Chemistry Resolved by Mass Spectrometry: Linking Field Measurements of  
926 Cloud Condensation Nuclei Activity to Organic Aerosol Composition. *Environ. Sci.  
927 Technol.* **2016**, *50* (20), 10823–10832. <https://doi.org/10.1021/acs.est.6b01675>.
- 928 (88) Zhang, H.; Lin, Y.-H.; Zhang, Z.; Zhang, X.; Shaw, S. L.; Knipping, E. M.; Weber, R. J.;  
929 Gold, A.; Kamens, R. M.; Surratt, J. D. Secondary Organic Aerosol Formation from  
930 Methacrolein Photooxidation: Roles of NO<sub>x</sub> Level, Relative Humidity and Aerosol Acidity.  
931 *Environ. Chem.* **2012**, *9* (3), 247–262. <https://doi.org/10.1071/EN12004>.
- 932 (89) Tanner, R. L.; Olszyna, K. J.; Edgerton, E. S.; Knipping, E.; Shaw, S. L. Searching for  
933 Evidence of Acid-Catalyzed Enhancement of Secondary Organic Aerosol Formation Using  
934 Ambient Aerosol Data. *Atmos. Environ.* **2009**, *43*, 3440–3444.  
935 <https://doi.org/10.1016/j.atmosenv.2009.03.045>.
- 936 (90) Jang, M.; Czoschke, N. M.; Lee, S.; Kamens, R. M. Heterogeneous Atmospheric Aerosol  
937 Production by Acid-Catalyzed Particle-Phase Reactions. *Science* **2002**, *298* (5594), 814–  
938 817. <https://doi.org/10.1126/science.1075798>.

- 939 (91) Weber, R. J.; Guo, H.; Russell, A. G.; Nenes, A. High Aerosol Acidity despite Declining  
940 Atmospheric Sulfate Concentrations over the Past 15 Years. *Nat. Geosci.* **2016**, *9* (April).  
941 <https://doi.org/10.1038/NGEO2665>.
- 942 (92) D'Ambro, E. L.; Schobesberger, S.; Gaston, C. J.; Lopez-Hilfiker, F. D.; Lee, B. H.; Liu,  
943 J.; Zelenyuk, A.; Bell, D.; Cappa, C. D.; Helgestad, T.; Li, Z.; Guenther, A.; Wang, J.; Wise,  
944 M.; Caylor, R.; Surratt, J. D.; Riedel, T.; Hyttinen, N.; Salo, V.-T.; Hasan, G.; Kurten, T.;  
945 Shilling, J. E.; Thornton, J. A. Chamber-Based Insights into the Factors Controlling  
946 Epoxydiol (IEPOX) Secondary Organic Aerosol (SOA) Yield, Composition, and Volatility.  
947 *Atmos. Chem. Phys.* **2019**, *19*, 11253–11265. <https://doi.org/10.5194/acp-19-11253-2019>.
- 948 (93) Kleindienst, T. E.; Lewandowski, M.; Offenberg, J. H.; Jaoui, M.; Edney, E. O. Ozone-  
949 Isoprene Reaction : Re-Examination of the Formation of Secondary Organic Aerosol.  
950 *Geophys. Res. Lett.* **2007**, *34* (1), 1–6. <https://doi.org/10.1029/2006GL027485>.
- 951 (94) Bateman, A. P.; Gong, Z.; Liu, P.; Sato, B.; Cirino, G.; Zhang, Y.; Artaxo, P.; Bertram, A.  
952 K.; Manzi, A. O.; Rizzo, L. V; Souza, R. A. F.; Zaveri, R. A.; Martin, S. T. Sub-Micrometre  
953 Particulate Matter Is Primarily in Liquid Form over Amazon Rainforest. *Nat. Geosci.* **2016**,  
954 *9* (January), 2–7. <https://doi.org/10.1038/NGEO2599>.
- 955 (95) Pajunoja, A.; Hu, W.; Leong, Y. J.; Taylor, N. F.; Miettinen, P.; Palm, B. B.; Mikkonen, S.;  
956 Collins, D. R.; Jimenez, J. L.; Virtanen, A. Phase State of Ambient Aerosol Linked with  
957 Water Uptake and Chemical Aging in the Southeastern US. *Atmos. Chem. Phys.* **2016**, *16*,  
958 11163–11176. <https://doi.org/10.5194/acp-16-11163-2016>.
- 959 (96) Isaacman, G. A.; Kreisberg, N. M.; Worton, D. R.; Hering, S. V; Goldstein, A. H. A  
960 Versatile and Reproducible Automatic Injection System for Liquid Standard Introduction:

- 961 Application to in-Situ Calibration. *Atmos. Meas. Tech.* **2011**, *4* (9), 1937–1942.  
962 <https://doi.org/10.5194/amt-4-1937-2011>.
- 963 (97) Zhang, H.; Yee, L. D.; Lee, B. H.; Curtis, M. P.; Worton, D. R.; Isaacman-VanWertz, G.;  
964 Offenberg, J. H.; Lewandowski, M.; Kleindienst, T. E.; Beaver, M. R.; Holder, A. L.;  
965 Lonneman, W. A.; Docherty, K. S.; Jaoui, M.; Pye, H. O. T.; Hu, W.; Day, D. A.;  
966 Campuzano-Jost, P.; Jimenez, J. L.; Guo, H.; Weber, R. J.; de Gouw, J.; Koss, A. R.;  
967 Edgerton, E. S.; Brune, W.; Mohr, C.; Lopez-Hilfiker, F. D.; Lutz, A.; Kreisberg, N. M.;  
968 Spielman, S. R.; Hering, S. V.; Wilson, K. R.; Thornton, J. A.; Goldstein, A. H.  
969 Monoterpenes Are the Largest Source of Summertime Organic Aerosol in the Southeastern  
970 United States. *Proc. Natl. Acad. Sci.* **2018**, *115* (9), 2038–2043.  
971 <https://doi.org/10.1073/pnas.1717513115>.
- 972 (98) Kamens, R. M.; Gery, M. W.; Jeffries, H. E.; Jackson, M.; Cole, E. I. Ozone-Isoprene  
973 Reactions: Product Formation and Aerosol Potential. *Int. J. Chem. Kinet.* **1982**, *14*, 955–  
974 975.
- 975
- 976

977 FOR TABLE OF CONTENTS ONLY



978